Composite pairing and superfluidity in a one-dimensional resonant Bose-Fermi mixture

Shimul Akhanjee,[1,2] Masahisa Tsuchiizu,[3] and Akira Furusaki[1,4]
[1]*Condensed Matter Theory Laboratory, RIKEN, Wako, Saitama 351-0198, Japan*
[2]*Department of Condensed Matter Physics and Materials Science, Brookhaven National Laboratory, Upton, New York 11973, USA*
[3]*Department of Physics, Nagoya University, Nagoya 464-8602, Japan*
[4]*RIKEN Center for Emergent Matter Science (CEMS), Wako, Saitama 351-0198, Japan*
(Received 1 April 2013; revised manuscript received 27 August 2013; published 16 October 2013)

We study the ground-state properties of one-dimensional mixtures of bosonic and fermionic atoms resonantly coupled to fermionic Feshbach molecules. When the particle densities of fermionic atoms and Feshbach molecules differ, the system undergoes various depletion transitions between binary and ternary mixtures as a function of the detuning parameter. However, when the particle densities of fermionic atoms and Feshbach molecules are identical, the molecular conversion and disassociation processes induce a gap in a sector of low-energy excitations, and the remaining system can be described by a two-component Tomonaga-Luttinger liquid. Using a bosonization scheme, we derive the effective low-energy Hamiltonian for the system, which has a similar form as that of the two-chain problem of coupled Tomonaga-Luttinger liquids. With the help of improved perturbative renormalization group analysis of the latter problem, we determine the ground-state phase diagram and find that it contains a phase dominated by composite superfluid or pairing correlations between the open and closed resonant channels.

DOI: 10.1103/PhysRevA.88.043620 PACS number(s): 03.75.Hh, 71.10.Pm, 71.10.Hf, 51.30.+i

I. INTRODUCTION

The Feshbach resonance [1], as experimentally realized in ultracold atoms and molecules in optical lattices, has made it possible to investigate the many-body physics of multicomponent quantum degenerate mixtures of fermions and/or bosons with interspecies interactions [2–6]. Operationally, a magnetic field near resonance can tune the energy splitting between different hyperfine configurations of atoms, yielding a tunable scattering amplitude with a magnitude that depends on the mismatch of the magnetic moments [7]. In this context, theoretical studies have introduced two primary interaction vertices: a short-ranged, one-channel density-density type interaction and a two-channel interaction that couples open-channel atoms to a molecular bound-state (MB) particle [8–10].

Recently, heteronuclear fermionic Feshbach molecules composed of bosonic ^{23}Na and fermionic ^{6}Li [11] and of bosonic ^{87}Rb and fermionic ^{40}K [12] have been observed experimentally and attracted the attention of theoretical studies [13–21] focusing on the competition between the condensed state of unpaired bosons and the degenerate MB particles with an additional Fermi surface. It has been argued that there can be depletion transitions [13,14,16] where one or more of the atomic or molecular species can be exhausted by driving the formation or disassociation of MB particles. Furthermore, if bosons are condensed, the spectrum can be directly diagonalized, yielding MB particles that are dressed by free atomic fermions, which form low-energy quasiparticles in a Fermi-liquid theory [21]. Additionally, the superfluidity of a paired state of a fermionic atom and a fermionic molecule, which is formed through attractive interactions mediated by the condensed and/or uncondensed bosons, has been predicted to occur [18]. However, it is questionable as to whether such features obtained by a mean-field approach can persist when strong quantum fluctuations are present, especially for atoms trapped in one-dimensional (1D) tubes.

There are many reliable analytical and numerical methods available for 1D systems [22,23]. In particular, the bosonization technique has been applied to one-channel systems with density-density type interactions, showing pairing and density-wave instabilities [24], polaronic phases [25–27], and competing orders [28]. The dominant phases exhibit variants of "paired" order parameters with algebraic decay or quasi-long-range order (QLRO) [24–27]. Systematic analysis has also been performed for a two-channel type model arising from atom-molecule mixture, expected for narrow resonances [29,30]; however, these investigations were primarily focused on the bosonic MB particles for two-component fermions in the context of the BEC-BCS crossover. The possibility of more complex pairing and superfluid orders that couple the open and closed fermionic channels has not been observed experimentally or discussed theoretically in detail.

In this paper, we study a general two-channel model of fermionic and bosonic atoms near a narrow Feshbach resonance where bosons, fermions, and molecules can coexist. Using a renormalization-group (RG) method based on the bosonization formalism, we obtain a low-energy theory and attempt to clarify the ground-state phase diagram, with an emphasis on the conditions that allow the pairing of the fermionic atoms and molecules across the Feshbach resonance. In doing so, we make use of the analogy to the two-chain problem of coupled Tomonaga-Luttinger liquids (TLL). The paper is organized as follows. In Sec. II, we introduce the model and examine the condition for ternary mixed phases of bosonic atoms, fermionic atoms, and fermionic molecules. In Sec. III, the ternary mixed phase is studied and possible order parameters are introduced to characterize QLRO. We determine the phase diagram for the case of an incommensurate density regime of fermions and molecules. In Sec. IV, the RG method is applied to analyze the low-energy properties, and in Sec. V, the phase diagram is determined for the commensurate density regime of fermions and molecules. Last, in Sec. VI we summarize our results in the conclusion. It

so happens that, given the mathematical form of the resonant interaction, we can draw on an RG approach applied to the spinless two-coupled chain, which is revisited in Appendix A. Finally, as a supplement, we present an alternative approach based on a gauge transformation procedure in Appendix B.

II. MODEL AND CONDITION FOR TERNARY MIXED PHASE

A. Model Hamiltonian

Our starting point is a coupled, two-channel model that describes a resonant scattering process, where free bosonic (b) and fermionic (f) atoms resonate into fermionic Feshbach molecules (ψ). The model Hamiltonian is given by

$$H = H_b + H_f + H_\psi + H_{3p}, \tag{2.1}$$

where

$$H_b = \int dx\, \Psi_b^\dagger(x)\left(-\frac{1}{2m_b}\frac{d^2}{dx^2} - \mu_b\right)\Psi_b(x) + \frac{1}{2}\int dx dx' V_{bb}(x-x')\rho_b(x)\rho_b(x'), \tag{2.2a}$$

$$H_f = \int dx\, \Psi_f^\dagger(x)\left(-\frac{1}{2m_f}\frac{d^2}{dx^2} - \mu_f\right)\Psi_f(x) + \frac{1}{2}\int dx dx' V_{ff}(x-x')\rho_f(x)\rho_f(x'), \tag{2.2b}$$

$$H_\psi = \int dx\, \Psi_\psi^\dagger(x)\left(-\frac{1}{2m_\psi}\frac{d^2}{dx^2} + \nu - \mu_\psi\right)\Psi_\psi(x) + \frac{1}{2}\int dx dx' V_{\psi\psi}(x-x')\rho_\psi(x)\rho_\psi(x'), \tag{2.2c}$$

$$H_{3p} = g_{3p}\int dx[\Psi_\psi^\dagger(x)\Psi_f(x)\Psi_b(x) + \text{H.c.}], \tag{2.2d}$$

and we have set $\hbar = 1$. The density operators are $\rho_s(x) = \Psi_s^\dagger(x)\Psi_s(x)$, $(s = b, f, \psi)$, where the field operators $\Psi_s(x)$ obey the usual commutation and anticommutation relations for bosons ($s = b$) and fermions ($s = f, \psi$). The Hamiltonian H_s $(s = b, f, \psi)$ consists of a kinetic energy term and an intraspecies density-density interaction term. The coupling g_{3p} in Eq. (2.2d) induces the conversion of bosonic (b) and fermionic (f) atoms into fermionic MB particles (ψ) and vice versa (disassociation) [8,9]. The individual particle numbers are not conserved; instead, the total numbers of bosonic and fermionic atoms,

$$\mathcal{N}_B = \int dx[\rho_b(x) + \rho_\psi(x)], \tag{2.3a}$$

$$\mathcal{N}_F = \int dx[\rho_f(x) + \rho_\psi(x)], \tag{2.3b}$$

are conserved quantities. It follows that the masses (m_s) and the chemical potentials (μ_s) obey the sum rules for mass conservation and chemical equilibrium,

$$m_b + m_f = m_\psi, \quad \mu_b + \mu_f = \mu_\psi, \tag{2.4}$$

and the detuning parameter ν in Eq. (2.2c) defines the energy splitting between the open and closed channels. The fermionic intraspecies couplings, $V_{ff}(x)$, and $V_{\psi\psi}(x)$, are assumed to be short-ranged, while the b atoms interact with each other through the coupling $V_{bb}(x)$. At strong repulsion, the boson system is described by an ordinary Tonks-Girardeau (TG) gas which behaves as free fermions.

B. Phase diagram in the limit of $g_{3p} \to 0$

Before proceeding to the many-body features of the model described by Eq. (2.1), it is important to first establish the range of physical parameters that allow the ternary coexistence of all atoms and molecules. For simplicity, we will consider the limit $g_{3p} \to 0$, with Tonks-Girardeau bosons [$V_{bb}(x) = g_b\delta(x)$ with $g_b \to +\infty$], and noninteracting fermions and molecules [$V_{ff}(x) = V_{\psi\psi}(x) = 0$]. As noted in Ref. [16], we can construct a set of dimensionless parameters $\mathcal{N}_F/\mathcal{N}_B$, m_f/m_b, and ν/T_0, where T_0 is the "Fermi" degeneracy temperature for hard-core bosons: $T_0 \equiv \pi^2\mathcal{N}_B^2/(2m_bL^2)$, with L being the system size.

Let us introduce the average particle density $\rho_s^0 = L^{-1}\int \rho_s(x)dx$ and the corresponding normalized quantity $\bar{\rho}_s \equiv L\rho_s^0/\mathcal{N}_B$. The conditions for the conserved total numbers of atoms [Eqs. (2.3)] are expressed as $1 = \bar{\rho}_b + \bar{\rho}_\psi$ and $\mathcal{N}_F/\mathcal{N}_B = \bar{\rho}_f + \bar{\rho}_\psi$, respectively. For hard core bosons, free fermions, and free molecules, the chemical potentials are given by $\mu_b = (k_F^b)^2/(2m_b)$, $\mu_f = (k_F^f)^2/(2m_f)$, and $\mu_\psi = (k_F^\psi)^2/(2m_\psi) + \nu$, where the "Fermi momenta" for each species are given by

$$k_F^s = \pi\rho_s^0. \tag{2.5}$$

The particle densities can be determined from the equilibrium condition of Eq. (2.4). In the ternary mixed phase of b, f, and ψ particles ($b + f + \psi$ phase), the density of molecules $\bar{\rho}_\psi$ is determined by the following equation:

$$(1-\bar{\rho}_\psi)^2 + \frac{1}{\bar{m}_f}(\bar{\mathcal{N}}_F - \bar{\rho}_\psi)^2 = \frac{1}{1+\bar{m}_f}(\bar{\rho}_\psi)^2 + \bar{\nu}, \tag{2.6}$$

where $\bar{\mathcal{N}}_F \equiv \mathcal{N}_F/\mathcal{N}_B$, $\bar{m}_f \equiv m_f/m_b$, and $\bar{\nu} \equiv \nu/T_0$. The densities for b atoms and f atoms are determined by $\bar{\rho}_b = 1 - \bar{\rho}_\psi$ and $\bar{\rho}_f = \bar{\mathcal{N}}_F - \bar{\rho}_\psi$, respectively, and the expected ν dependence is shown in Fig. 1. Notice that in the case

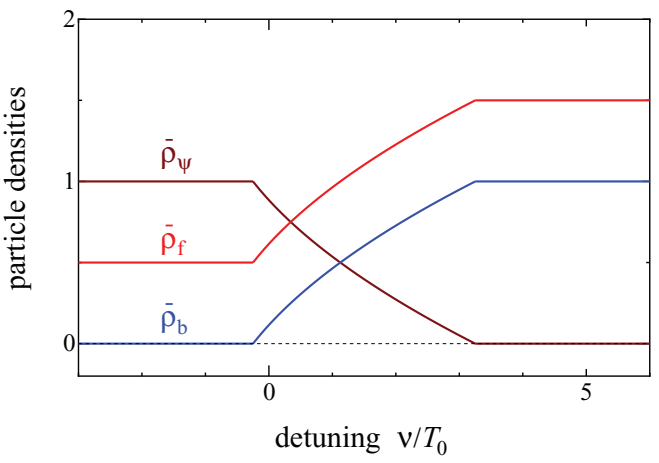

FIG. 1. (Color online) The normalized particle densities $\bar{\rho}_s \equiv L\rho_s^0/\mathcal{N}_B$ as a function of the detuning parameter ν. In this figure, we choose $m_b = m_f$ and $\mathcal{N}_F/\mathcal{N}_B = 3/2$. At $\nu/T_0 = 11/32$, the densities of fermions and molecules become equal, $\bar{\rho}_f = \bar{\rho}_\psi = 3/4$.

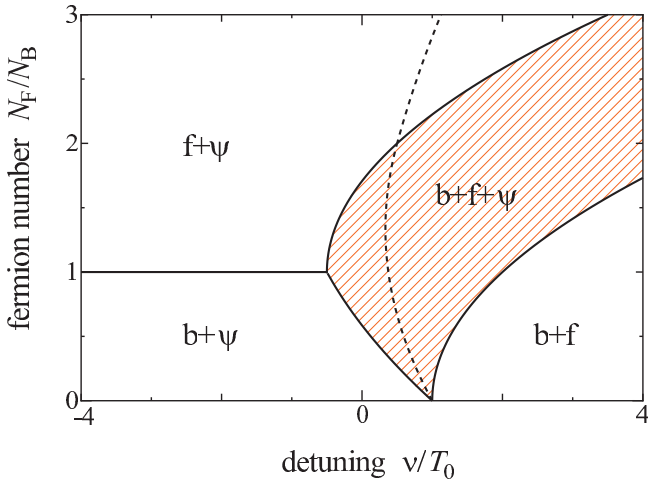

FIG. 2. (Color online) Phase diagram in terms of the detuning parameter ν and the fermion number $\mathcal{N}_F$ for the case of equal masses $m_b = m_f$. The ternary mixed state of bosonic atoms, fermionic atoms, and Feshbach molecules is realized in the region denoted by "$b+f+\psi$." The regions denoted by "$f+\psi$," "$b+\psi$," and "$b+f$" represent the fermion-molecule, boson-molecule, and boson-fermion binary mixed phases, respectively. Along the dashed line, the densities of fermions and molecules become equal, $\bar{\rho}_f = \bar{\rho}_\psi$.

of sufficiently strong positive detuning, the ψ particle is completely depleted and only the b and f atoms remain. We thus label this binary mixture the "$b+f$" phase; effects of possible heteroatomic interactions in this regime have been analyzed in the literature [24–28,31,32], where it has been pointed out that the excitation spectrum can have a gap and the pairing fluctuations are enhanced when the particle densities of two kinds of atoms become equal. On the other hand, the MB particles become stable for sufficiently strong negative detuning; for $\mathcal{N}_F/\mathcal{N}_B < 1$ (>1), either b or f atoms coexist with the ψ particles and the resulting binary mixtures are labeled "$b+\psi$" and "$f+\psi$" phases, respectively.

The phase diagram in terms of the detuning parameter ν and the total fermion number $\mathcal{N}_F$ is shown in Fig. 2, which can be contrasted with the corresponding phase diagram in the three-dimensional (3D) case (see Fig. 3 in Ref. [13], Fig. 3 in Ref. [16], and also Fig. 1 in Ref. [18]), where the Bose-Einstein condensate (BEC) proliferates everywhere except for the small ν and large $\mathcal{N}_F$ region corresponding to the $f+\psi$ phase in Fig. 2. In the present 1D case, no BEC can occur in any parameter region, but a "Fermi surface" of the b atoms can be observed instead. With this in mind, we find qualitative agreement with our phase diagram for 1D mixtures and that for 3D mixtures. The densities of fermions and molecules become identical ($\bar{\rho}_f = \bar{\rho}_\psi$) in both ternary and binary mixed phases for a particular $\bar{\nu}$, satisfying

$$\bar{\nu} = \begin{cases} 1 - \bar{\mathcal{N}}_F + \frac{1+\bar{m}_f+\bar{m}_f^2}{4\bar{m}_f(1+\bar{m}_f)}\bar{\mathcal{N}}_F^2 & (b+f+\psi \text{ phase}), \\ \frac{1}{4}\left(\frac{1}{\bar{m}_f} - \frac{1}{1+\bar{m}_f}\right)\bar{\mathcal{N}}_F^2 & (f+\psi \text{ phase}), \end{cases} \tag{2.7}$$

which is represented by the dashed line in Fig. 2. The analysis given in Ref. [24] may be applied to the case $\bar{\rho}_f = \bar{\rho}_\psi$ in the $f+\psi$ phase. However, the spectrum for the case $\bar{\rho}_f = \bar{\rho}_\psi$ in the $b+f+\psi$ phase has not yet been analyzed so far. In the following sections, we study phases realized inside the $b+f+\psi$ phase upon turning on the g_{3p} coupling.

III. BOSONIZATION

A. Bosonized Hamiltonian

The dominant low-energy behavior of the model defined by Eqs. (2.2) can be studied by using a harmonic fluid representation, where the single-particle dispersion relations are linearized near the "Fermi" points. In the problem of BEC-BCS crossover in one dimension, a two-channel model of two-component fermions that dimerize into bosonic molecules has been previously analyzed by means of the bosonization method in Refs. [29] and [30]. Because of the different statistics of particles, the bosonization analysis of the present model will reveal different phases.

In terms of the bosonic phase fields $\phi_s(x)$, the density operators can be expressed as [22,23,33]

$$\rho_s(x) = \rho_s^0 - \frac{1}{\pi}\frac{d\phi_s(x)}{dx} + \rho_s^0 \sum_{m\neq 0} e^{2im[\pi\rho_s^0 x - \phi_s(x)]}, \tag{3.1}$$

where ρ_s^0 is the equilibrium density and the summation is over nonzero integer m. The field operators for the respective particles are represented as [22,23,33]

$$\Psi_b(x) = \frac{1}{\sqrt{2\pi\alpha}} \sum_{n\in\mathbb{Z}} e^{in[2\pi\rho_b^0 x - 2\phi_b(x)] + i\theta_b(x)}, \tag{3.2a}$$

$$\Psi_f^{L/R}(x) = \frac{\xi_f}{\sqrt{2\pi\alpha}} e^{\mp i[\pi\rho_f^0 x - \phi_f(x)] + i\theta_f(x)}, \tag{3.2b}$$

$$\Psi_\psi^{L/R}(x) = \frac{\xi_\psi}{\sqrt{2\pi\alpha}} e^{\mp i[\pi\rho_\psi^0 x - \phi_\psi(x)] + i\theta_\psi(x)}, \tag{3.2c}$$

where α is a short-distance cutoff. The field operators Ψ_s^L and Ψ_s^R ($s = f,\psi$) represent the left-moving and right-moving chiral branches of fermionic particles, respectively. The Klein factors ξ_f and ξ_ψ, satisfying $\{\xi_s,\xi_{s'}\} = 2\delta_{s,s'}$ and $\xi_s^\dagger = \xi_s$, are introduced in order to retain the anticommutation relation between f and ψ particles. $\theta_s(x)$ are dual fields to $\phi_s(x)$ and obey $[\phi_s(x),\theta_{s'}(x')] = i\pi\delta_{s,s'}\Theta(-x+x')$, where $\Theta(x)$ is the Heaviside step function, i.e., $\Theta(x) = 1$ for $x > 0$, $\Theta(0) = \frac{1}{2}$, and $\Theta(x) = 0$ for $x < 0$. By introducing the conjugate momenta $\Pi_s(x) = (1/\pi)\partial_x\theta_s(x)$, a generic TLL Hamiltonian for each component is expressed as

$$H_s = \frac{u_s}{2\pi}\int dx \left\{ K_s[\pi\Pi_s(x)]^2 + \frac{1}{K_s}[\partial_x\phi_s(x)]^2 \right\}. \tag{3.3}$$

The parameters u_s and K_s are velocities and TLL parameters, respectively, which depend on the precise forms of microscopic intraspecies interactions. We will consider the general case where $0 < K_{s=b,f,\psi} < \infty$. The noninteracting limits $V_{bb} \to 0$ and V_{ff}, $V_{\psi\psi} \to 0$ correspond to $K_b = \infty$ and $K_{s=f,\psi} = 1$, respectively. By tuning $g_b \to \infty$, the system enters the TG regime at $K_b \gtrsim 1$ [23,33]. For specific realizations of optical lattice systems, the commensurability of the Bose-Hubbard interaction allows the possibility of tuning into the regime $K_b < 1$, when V_{bb} is long ranged [23,33].

After substituting the bosonized form of $\Psi_s(x)$ defined in Eqs. (3.2) into Eq. (2.2d) and keeping only the $n = 0$ term for

Ψ_b, we obtain

$$H_{3p} = -i\tilde{g}_{3p}\int dx\cos[\theta_b(x)+\theta_f(x)-\theta_\psi(x)] \times \sin[\phi_f(x)-\phi_\psi(x)-\delta k_F x], \tag{3.4}$$

where $\delta k_F \equiv k_F^f - k_F^\psi$ and $\tilde{g}_{3p} = 4g_{3p}(2\pi\alpha)^{-3/2}$. In deriving Eq. (3.4) we have discarded terms like $\tilde{g}_{3p}\sin(\theta_b+\theta_f-\theta_\psi)\cos(2k_F x-\phi_f-\phi_\psi)$, which are strongly irrelevant in the RG sense because they have spatial oscillations with the wave number $2k_F \equiv k_F^f + k_F^\psi = \pi\mathcal{N}_F/L$. Furthermore, we have replaced $\xi_f\xi_\psi$ with $+i$, because the product of the two Klein factors is a constant of motion [the identity $(\xi_f\xi_\psi)^2=-1$ implies either $\xi_f\xi_\psi=+i$ or $-i$, and we have chosen the former]. We will use the same sign convention when we derive bosonized form of order parameters.

In the incommensurate case ($\delta k_F \neq 0$), the g_{3p} interaction [Eq. (3.4)] is irrelevant in the RG sense. The analysis of the previous section is then applicable, and the phase diagram therefore can be determined as in the previous section, with various depletion transitions occurring between binary and ternary mixture phases. On the other hand, Eq. (3.4) has a dramatically different effect for the commensurate case ($\delta k_F = 0$), which is satisfied along the dashed line in Fig. 2. In this case, sinusoidal potentials can lock a particular phase variable (θ_s or ϕ_s), and a competition of various orders due to the phase locking must be studied by performing a RG analysis.

B. Order parameters

In the context of quantum mixtures, composite "pairing" correlations have been previously introduced in the literature and will be extended here to a more comprehensive list of possible order parameters. First, the conventional $2k_F$ density-wave (DW) order parameters are given by

$$\mathcal{O}_b^{\rm DW}(x) = \Psi_b^\dagger(x)\Psi_b(x) \simeq e^{i(2k_F^b x-2\phi_b)}, \tag{3.5a}$$

$$\mathcal{O}_f^{\rm DW}(x) = \Psi_f^{L\dagger}(x)\Psi_f^R(x) \simeq e^{i(2k_F^f x-2\phi_f)}, \tag{3.5b}$$

$$\mathcal{O}_\psi^{\rm DW}(x) = \Psi_\psi^{L\dagger}(x)\Psi_\psi^R(x) \simeq e^{i(2k_F^\psi x-2\phi_\psi)}. \tag{3.5c}$$

Here (and below) we have dropped unimportant numerical prefactors. In analogy with order parameters in the spinless two-coupled chain system [see Eq. (A4a)], we introduce the out-of-phase DW state of f and ψ particles,

$$\mathcal{O}_{f\psi}^{\rm DW}(x) = \Psi_f^{L\dagger}(x)\Psi_f^R(x) - \Psi_\psi^{L\dagger}(x)\Psi_\psi^R(x) \simeq e^{i2k_F x-i(\phi_f+\phi_\psi)}\sin(\phi_f-\phi_\psi-\delta k_F x). \tag{3.5d}$$

Next, the order parameters for the superfluidity (SF) of bosons, p-wave-paired fermions, and p-wave-paired molecules are given by

$$\mathcal{O}_b^{\rm SF}(x) = \Psi_b(x) \simeq e^{i\theta_b}, \tag{3.5e}$$

$$\mathcal{O}_{ff}^{\rm SF}(x) = \Psi_f^L(x)\Psi_f^R(x) \simeq e^{i2\theta_f}, \tag{3.5f}$$

$$\mathcal{O}_{\psi\psi}^{\rm SF}(x) = \Psi_\psi^L(x)\Psi_\psi^R(x) \simeq e^{i2\theta_\psi}. \tag{3.5g}$$

We will also consider the p-wave-paired SF state composed of f and ψ particles,

$$\mathcal{O}_{f\psi}^{\rm SF}(x) = \Psi_f^L(x)\Psi_\psi^R(x) - \Psi_f^R(x)\Psi_\psi^L(x) \simeq e^{i(\theta_f+\theta_\psi)}\sin(\phi_f-\phi_\psi-\delta k_F x), \tag{3.5h}$$

which is odd under the parity transformation, $L\leftrightarrow R$, and therefore can be classified as p-wave pairing. Moreover, this order parameter can be identified with the interchain pairing SCd state in the two-coupled spinless chain problem [see Eq. (A4c)], where f and ψ can be replaced by the two-chain indices.

Earlier work in Ref. [34] investigated the phase diagram of interacting "$b+f$" binary mixtures near the commensurate point $\bar{\rho}_b = \bar{\rho}_f$, where the composite p-wave superfluidity $\sim\Psi_b^2\Psi_f^L\Psi_f^R$ was shown to have dominant QLRO correlations. In the ternary system studied here, similar orders can persist,

$$\mathcal{O}_{bff+b^\dagger\psi\psi}^{\rm SF}(x) = \Psi_b\Psi_f^L\Psi_f^R + \Psi_b^\dagger\Psi_\psi^L\Psi_\psi^R \simeq e^{i(\theta_f+\theta_\psi)}\cos(\theta_b+\theta_f-\theta_\psi), \tag{3.5i}$$

which describes the p-wave pairing of two fermionic (f or ψ) particles combined with a single b atom. Note that the two composite operators in Eq. (3.5i), $\Psi_b\Psi_f^L\Psi_f^R$ and $\Psi_b^\dagger\Psi_\psi^L\Psi_\psi^R$, annihilate equal numbers of fermionic and bosonic atoms (including the ones forming a molecule), as seen from the commutation relations $[\mathcal{N}_B,\mathcal{O}_{bff+b^\dagger\psi\psi}^{\rm SF}] = -\mathcal{O}_{bff+b^\dagger\psi\psi}^{\rm SF}$ and $[\mathcal{N}_F,\mathcal{O}_{bff+b^\dagger\psi\psi}^{\rm SF}] = -2\mathcal{O}_{bff+b^\dagger\psi\psi}^{\rm SF}$. This order parameter corresponds to the intrachain SCs pairing in the two-coupled chain problem [see Eq. (A4d)].

In addition, we consider other composite order parameters defined by

$$\mathcal{O}_{b^\dagger f^\dagger\psi}^{\rm ph1}(x) = \Psi_b^\dagger\Psi_f^{L\dagger}\Psi_\psi^L - \Psi_b\Psi_\psi^{R\dagger}\Psi_f^R \simeq e^{i\delta k_F x-i(\phi_f-\phi_\psi)}\sin(\theta_b+\theta_f-\theta_\psi) + e^{i(-2k_F^b+\delta k_F)x+i(2\phi_b-\phi_f+\phi_\psi)} \times \cos(\theta_b+\theta_f-\theta_\psi), \tag{3.5j}$$

$$\mathcal{O}_{b^\dagger f^\dagger\psi}^{\rm ph2}(x) = \Psi_b^\dagger\Psi_f^{L\dagger}\Psi_\psi^R - \Psi_b\Psi_\psi^{L\dagger}\Psi_f^R \simeq e^{i2k_F x-i(\phi_f+\phi_\psi)}\cos(\theta_b+\theta_f-\theta_\psi), \tag{3.5k}$$

which represent the particle-hole combinations of f and ψ fermions. These operators are composed of the products of three field operators, $\Psi_b^\dagger\Psi_f^\dagger\Psi_\psi$ and $\Psi_b\Psi_\psi^\dagger\Psi_f$, which are similar in form to the g_{3p} term of Eq. (2.2d) but asymmetrical in the L,R branches. The second bosonized contribution in Eq. (3.5j), coming from the $n=-1$ contribution in Eq. (3.2a), can become a dominant order parameter for some parameter regime, as will be shown later. We also note that the order parameter in Eq. (3.5k) corresponds to the "orbital antiferromagnetic state" in the two-coupled chain problem, in which circulating currents flow between the two chains, if the f and ψ indices are regarded as chain indices [see Eq. (A4b)].

C. Ground states in the incommensurate case

When $\delta k_F \neq 0$, the g_{3p} interaction of Eq. (3.4) oscillates in space and does not affect the low-energy spectrum. Thus we can set $g_{3p}=0$ in the low-energy limit, and the system is described as a three-component TLL, in which the b, f, and ψ particles are decoupled and the correlation functions exhibit

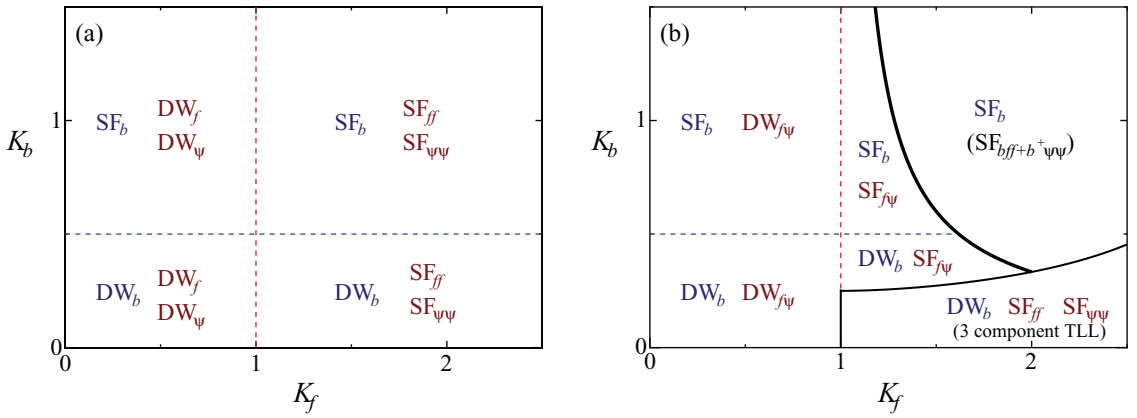

FIG. 3. (Color online) Phase diagram of Hamiltonian (2.1) for the incommensurate case $\rho_f \neq \rho_\psi$ (a) and the commensurate case $\rho_f = \rho_\psi$ (b). For simplicity we set $u_b = u_f = u_\psi$ and $K_\psi = K_f$. The regions labeled by DW and SF represent phases with the dominant density-wave and superfluid correlations, respectively. The dominant correlation crosses over from DW to SF or vice versa across the dashed lines. (b) In the phase denoted by "(3 component TLL)," all the couplings G_{3p}, G_ϕ, and G_θ are irrelevant in the RG sense. The boundary between the phases of relevant G_ϕ and that of relevant G_θ is shown by the thick solid line at which the system undergoes a quantum phase transition. On the left-hand (right-hand) side of the thick solid line, the coupling G_ϕ (G_θ) becomes relevant.

algebraic decay. For example, the correlators for the b particles are given by

$$\langle \mathcal{O}_b^{\mathrm{SF}}(x)\,\mathcal{O}_b^{\mathrm{SF}\dagger}(0)\rangle_0 \sim x^{-1/(2K_b)}, \tag{3.6a}$$

$$\langle \mathcal{O}_b^{\mathrm{DW}}(x)\,\mathcal{O}_b^{\mathrm{DW}\dagger}(0)\rangle_0 \sim x^{-2K_b} e^{i2k_F^b x}. \tag{3.6b}$$

We find that the superfluidity correlation dominates over the density-wave correlation when $K_b > 1/2$. Similarly, the correlation functions for the p-wave superfluidity and the density-wave of the f and ψ particles exhibit algebraic decay,

$$\langle \mathcal{O}_{ss}^{\mathrm{SF}}(x)\,\mathcal{O}_{ss}^{\mathrm{SF}\dagger}(0)\rangle_0 \sim x^{-2/K_s}, \tag{3.7a}$$

$$\langle \mathcal{O}_s^{\mathrm{DW}}(x)\,\mathcal{O}_s^{\mathrm{DW}\dagger}(0)\rangle_0 \sim x^{-2K_s} e^{i2k_F^s x}, \tag{3.7b}$$

where $s = f,\psi$. The dominant correlation for fermions changes between the superfluidity and density-wave orders at $K_s = 1$. In Fig. 3(a) we show the phase diagram in the parameter space of K_s ($s = b,f,\psi$), which is obtained by identifying the dominant QLRO among those in Eqs. (3.6) and (3.7).

IV. RENORMALIZATION IN THE COMMENSURATE CASE

When $\delta k_F \simeq 0$, the effects of the sinusoidal potential (3.4) can be analyzed using RG techniques [33]. Apparently, the form of Eq. (3.4) contains dual fields which do not commute $[\theta_b + \theta_f - \theta_\psi, \phi_f - \phi_\psi] \neq 0$. This type of interaction has been analyzed in the context of two TLL chains coupled by one-particle interchain hopping [35,36], where it has been confirmed that higher-order corrections are crucial to determine the low-energy spectrum of the two TLL chains [37]. We thus can expect that interactions generated by RG transformation should similarly be taken into account in our model.

In order to properly derive the RG equations and to determine the ground-state phase diagram for the Hamiltonian including the potential as Eq. (3.4), we have to pay special attention to the commutative properties of the phase fields, besides the Klein factors. In Appendix A, we analyze the two-coupled chain system on the basis of the present bosonization scheme and verify that the correct results [38] can be derived. In Ref. [38], the interchain hopping term was treated nonperturbatively and the phase diagram was determined. In Appendix B, we analyze the present model (2.1) using the method of Ref. [38] and observe that the consistent results can be obtained.

In this section we set $u_b = u_f = u_\psi (\equiv u)$ for simplicity. The Euclidean action of the system is given by $S = S_0 + S_{I,0} + S_{I,1} + S_{I,2} + S_{I,3}$ with

$$S_0 = \sum_s \frac{1}{2\pi K_s} \int d^2r (\nabla\phi_s)^2, \tag{4.1a}$$

$$S_{I,0} = \sum_{s\neq s'} \frac{G_{ss'}}{2\pi} \int d^2r\, (\nabla\phi_s)(\nabla\phi_{s'}), \tag{4.1b}$$

$$S_{I,1} = \frac{G_{3p}}{i\pi} \int \frac{d^2r}{\alpha^2} \cos(\theta_b + \theta_f - \theta_\psi) \sin(\phi_f - \phi_\psi), \tag{4.1c}$$

$$S_{I,2} = \frac{G_\phi}{\pi} \int \frac{d^2r}{\alpha^2} \cos(2\phi_f - 2\phi_\psi), \tag{4.1d}$$

$$S_{I,3} = \frac{G_\theta}{\pi} \int \frac{d^2r}{\alpha^2} \cos(2\theta_b + 2\theta_f - 2\theta_\psi), \tag{4.1e}$$

where $\boldsymbol{r} = (x, u\tau)$, $\nabla = (\partial_x, u^{-1}\partial_\tau)$, $d^2r = u dx d\tau$, and $G_{3p} = \pi\alpha^2 \tilde{g}_{3p}/u$. Although the extra terms G_ϕ, G_θ, G_{bf}, $G_{b\psi}$, and $G_{f\psi}$, are absent in the original Hamiltonian, they are generated through the RG process [35].

In this paper, we adopt the momentum-space RG method [39] by introducing the momentum space cutoff Λ. The RG equations can be obtained by integrating out the high-momentum components $\Lambda' < |\boldsymbol{k}| < \Lambda$, where $\Lambda' = \Lambda(1 - dl)$ is the reduced cutoff ($dl = -d\Lambda/\Lambda$) and $\boldsymbol{k} = (k, \omega/u)$ with the frequency ω. Accordingly, the phase fields $\phi_s(\boldsymbol{r})$ are split into two components $\phi_s(\boldsymbol{r}) = \phi_s'(\boldsymbol{r}) + h_s(\boldsymbol{r})$ [39], where

$\phi'_s(\boldsymbol{r})$ is the field having components in lower momentum $0 < |\boldsymbol{k}| < \Lambda'$ and $h_s(x)$ has higher momentum components $\Lambda' < |\boldsymbol{k}| < \Lambda$. The free propagators for these fields are given by

$$\langle \phi'_s(\boldsymbol{r})\phi'_s(\boldsymbol{0})\rangle = \frac{K_s}{2}\bar{g}(r) = \frac{K_s}{2}\int_0^\infty \frac{dk}{k} J_0(kr) f(k/\Lambda'), \tag{4.2}$$

$$\begin{aligned}\langle h_s(\boldsymbol{r})h_s(\boldsymbol{0})\rangle &= \frac{K_s}{2}\delta g(r) \\ &= \frac{K_s}{2}\int_0^\infty \frac{dk}{k} J_0(kr)[f(k/\Lambda) - f(k/\Lambda')],\end{aligned} \tag{4.3}$$

where $r = |\boldsymbol{r}|$ and $J_0(z)$ is the Bessel function of the first kind. With the smooth cutoff function $f(p) = c^2/(p^2 + c^2)$ [40], we have the correlation functions $\langle[\phi'_s(\boldsymbol{r}) - \phi'_s(\boldsymbol{0})]^2\rangle = K_s \ln(e^\gamma c\Lambda'|\boldsymbol{r}|/2)$ and $\delta g(r) = c\Lambda r K_1(c\Lambda r) dl$ for $c\Lambda r \gg 1$, where $K_1(z)$ is the modified Bessel function. The constant c is taken as $c = 2e^{-\gamma}/(\Lambda\alpha)$ in order to reproduce the asymptotic form $\langle[\phi_s(\boldsymbol{r}) - \phi_s(\boldsymbol{0})]^2\rangle = K_s \ln(|\boldsymbol{r}|/\alpha)$ for $|\boldsymbol{r}| \to \infty$. The derivation of one-loop RG equations proceeds similarly to the case of the two-coupled chain system explained in Appendix A. By exploiting the commutation relation $[\phi_s(x),\theta_{s'}(x')] = i\pi\delta_{s,s'}\Theta(-x + x')$ and the normal ordering procedure for the operator-product expansion [33,41], we eventually obtain the following one-loop RG equations:

$$\begin{aligned}\frac{dG_{3p}}{dl} &= \Big(2 - \frac{1}{4K_b} - \frac{1}{4K_f} - \frac{1}{4K_\psi} - \frac{K_f}{4} - \frac{K_\psi}{4} - \frac{1}{2}G_{bf} \\ &\quad + \frac{1}{2}G_{b\psi} + \frac{1}{2}G_{f\psi} - \frac{1}{2}G_{f\psi}K_fK_\psi\Big)G_{3p},\end{aligned} \tag{4.4a}$$

$$\begin{aligned}\frac{dG_\phi}{dl} &= (2 - K_f - K_\psi - 2G_{f\psi}K_fK_\psi)G_\phi \\ &\quad + \frac{1}{4}G_{3p}^2 A_1\big(\big(K_b^{-1} + K_f^{-1} + K_\psi^{-1} - K_f - K_\psi\big)/4\big),\end{aligned} \tag{4.4b}$$

$$\begin{aligned}\frac{dG_\theta}{dl} &= \Big(2 - \frac{1}{K_b} - \frac{1}{K_f} - \frac{1}{K_\psi} - 2G_{bf} \\ &\quad + 2G_{b\psi} + 2G_{f\psi}\Big)G_\theta \\ &\quad - \frac{1}{4}G_{3p}^2 A_1\big(\big(K_f + K_\psi - K_b^{-1} - K_f^{-1} - K_\psi^{-1}\big)/4\big),\end{aligned} \tag{4.4c}$$

$$\frac{dK_b}{dl} = +G_\theta^2 A_2\big(K_b^{-1} + K_f^{-1} + K_\psi^{-1}\big), \tag{4.4d}$$

$$\begin{aligned}\frac{dK_f}{dl} &= -G_\phi^2 K_f^2 A_2(K_f + K_\psi) \\ &\quad + G_\theta^2 A_2\big(K_b^{-1} + K_f^{-1} + K_\psi^{-1}\big),\end{aligned} \tag{4.4e}$$

$$\begin{aligned}\frac{dK_\psi}{dl} &= -G_\phi^2 K_\psi^2 A_2(K_f + K_\psi) \\ &\quad + G_\theta^2 A_2\big(K_b^{-1} + K_f^{-1} + K_\psi^{-1}\big),\end{aligned} \tag{4.4f}$$

$$\frac{dG_{bf}}{dl} = +\frac{G_\theta^2}{K_bK_f} A_2\big(K_b^{-1} + K_f^{-1} + K_\psi^{-1}\big), \tag{4.4g}$$

$$\frac{dG_{b\psi}}{dl} = +\frac{G_\theta^2}{K_bK_\psi} A_2\big(K_b^{-1} + K_f^{-1} + K_\psi^{-1}\big), \tag{4.4h}$$

$$\begin{aligned}\frac{dG_{f\psi}}{dl} &= -G_\phi^2 A_2(K_f + K_\psi) \\ &\quad + \frac{G_\theta^2}{K_fK_\psi} A_2\big(K_b^{-1} + K_f^{-1} + K_\psi^{-1}\big),\end{aligned} \tag{4.4i}$$

where we have defined

$$A_1(\beta)dl \equiv 2\beta\int_0^\infty \frac{dr}{\alpha}\frac{r}{\alpha}\delta g(r)e^{-2\beta[\bar{g}(0)-\bar{g}(r)]}, \tag{4.5a}$$

$$A_2(\beta)dl \equiv 2\beta\int_0^\infty \frac{dr}{\alpha}\frac{r^3}{\alpha^3}\delta g(r)e^{-2\beta[\bar{g}(0)-\bar{g}(r)]}. \tag{4.5b}$$

The exponential factors in the right-hand side of Eqs. (4.5) appear as a result of normal ordering in operator-product expansions [33,41]; for example,

$$\begin{aligned}&\cos[p\phi'_s(\boldsymbol{r}_1) + q\phi'_s(\boldsymbol{r}_2)] \\ &= :\cos[p\phi'_s(\boldsymbol{r}_1) + q\phi'_s(\boldsymbol{r}_2)]: e^{-\frac{1}{2}(p^2+q^2)\langle\phi'^2_s\rangle - pq\langle\phi'_s(\boldsymbol{1})\phi'_s(\boldsymbol{2})\rangle} \\ &\approx :\cos[(p+q)\phi'_s(\boldsymbol{R})]: e^{-\frac{1}{2}(p^2+q^2)\langle\phi'^2_s\rangle - pq\langle\phi'_s(\boldsymbol{1})\phi'_s(\boldsymbol{2})\rangle} \\ &= \cos[(p+q)\phi'_s(\boldsymbol{R})]\, e^{\frac{1}{2}[(p+q)^2-(p^2+q^2)]\langle\phi'^2_s\rangle - pq\langle\phi'_s(\boldsymbol{1})\phi'_s(\boldsymbol{2})\rangle} \\ &= \cos[(p+q)\phi'_s(\boldsymbol{R})]\, e^{\frac{1}{2}pqK[\bar{g}(0)-\bar{g}(r_{12})]},\end{aligned} \tag{4.6}$$

where $\boldsymbol{R} = (\boldsymbol{r}_1 + \boldsymbol{r}_2)/2$ and $r_{12} = |\boldsymbol{r}_1 - \boldsymbol{r}_2|$. We have used the short-hand notations $\boldsymbol{1} = \boldsymbol{r}_1$ and $\boldsymbol{2} = \boldsymbol{r}_2$. We note that $A_1(\beta) \approx e^{2\gamma}\beta$ for small β, and $A_1(1) = A_2(2) = 1$, where γ is the Euler-Mascheroni constant. One can neglect the velocity renormalization up to one-loop order. The initial values of the RG equations are given by $G_{3p}(0) = G_{3p}$, $K_s(0) = K_s$, and $G_{ss'}(0) = G_\phi(0) = G_\theta(0) = 0$.

Diagrammatic representations for the G_{3p}, G_ϕ, and G_θ terms are shown in Fig. 4. The G_ϕ coupling is a four-point vertex representing interactions between f and ψ particles, while the G_θ coupling is a six-point vertex for a two-molecule conversion from two b and two f particles. Low-order contributions to G_ϕ and G_θ are also shown in Fig. 4. The

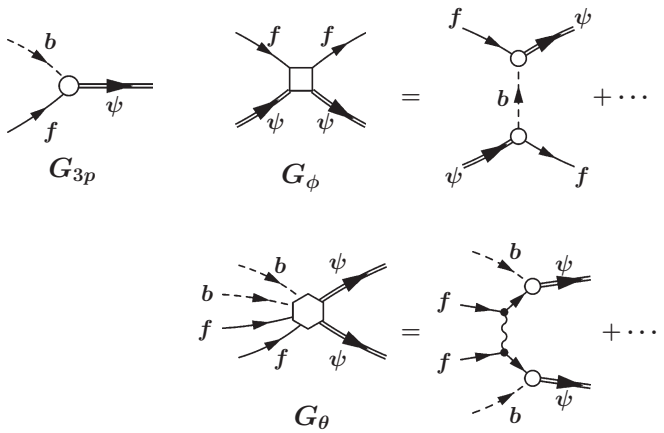

FIG. 4. Diagrammatic representation of the G_{3p}, G_ϕ, and G_θ terms, and low-order contributions to G_ϕ and G_θ. The dashed, sold, and double lines represent the boson, fermion, and molecule propagators, respectively. The wavy line represents the intraspecies density-density interaction.

lowest-order contribution to the G_ϕ coupling comes from the effective interaction mediated by b atoms. Pairing between fermions (f) and molecules (ψ) induced by such boson- (b) mediated interaction has been suggested in Ref. [18]. We will contrast this paper with our work in more detail later.

Since $[\phi_f - \phi_\psi, \theta_b + \theta_f - \theta_\psi] \neq 0$, the phase variables $\phi_f - \phi_\psi$ and $\theta_b + \theta_f - \theta_\psi$ cannot be locked simultaneously. This means that there should be two distinct phases separated by a quantum phase transition, a phase where $\phi_f - \phi_\psi$ is locked by the G_ϕ term and a phase where $\theta_b + \theta_f - \theta_\psi$ is locked by the G_θ term, in addition to a three-component TLL phase where none of the phase fields are locked. Here we obtain the phase diagram by comparing the scaling dimensions, which we denote by dim[ ], of the operators for the couplings G_{3p}, G_ϕ, and G_θ. We ignore renormalization of K_b, K_f, and K_ψ for weak g_{3p}, because the right-hand side of Eqs. (4.4d)–(4.4f) are of order g_{3p}^4. The scaling dimensions of the sinusoidal potential operators are found from Eqs. (4.4a)–(4.4c) as

$$\begin{aligned} \dim[G_{3p}] &= \frac{1}{4}\left(\frac{1}{K_b} + \frac{1}{K_f} + \frac{1}{K_\psi} + K_f + K_\psi\right), \\ \dim[G_\phi] &= K_f + K_\psi, \\ \dim[G_\theta] &= \frac{1}{K_b} + \frac{1}{K_f} + \frac{1}{K_\psi}. \end{aligned} \tag{4.7}$$

In the case when three inequalities, $\dim[G_{3p}] > 2$, $\dim[G_\phi] > 2$, and $\dim[G_\theta] > 2$, are simultaneously satisfied, all the locking potential operators are irrelevant, and, consequently, we have a three-component TLL phase. This is the case for large K_f and K_ψ and small K_b. Otherwise, either the coupling G_ϕ or G_θ becomes relevant and flows to strong coupling at low energy.

We observe from Eqs. (4.4b) and (4.4c) that the condition

$$K_f + K_\psi = \frac{1}{K_b} + \frac{1}{K_f} + \frac{1}{K_\psi} \tag{4.8}$$

defines the particular case where the scaling dimensions $\dim[G_\phi]$ and $\dim[G_\theta]$ become identical and the factor A_1 in the second terms of the right-hand side of Eqs. (4.4b) and (4.4c) vanishes. Thus, Eq. (4.8) determines the phase boundary between the phase where the G_ϕ operator is relevant and the phase where the G_θ operator is relevant. In the case where $K_f + K_\psi < K_b^{-1} + K_f^{-1} + K_\psi^{-1}$, the coupling G_ϕ is relevant and renormalized to strong coupling with $G_\phi > 0$. We note that the positive G_ϕ coupling implies *repulsive* density-density interactions between f and ψ particles. On the other hand, in the opposite case where $K_f + K_\psi < K_b^{-1} + K_f^{-1} + K_\psi^{-1}$, the coupling G_θ is relevant and renormalized to strong coupling with $G_\theta < 0$.

The resulting phase diagram is shown in Fig. 3(b), for which the nature of the ground state in each phase is discussed in the next section.

V. PHASE DIAGRAM IN THE COMMENSURATE CASE

In the preceding section we determined the phase boundaries in the phase diagram that admit quantum phase transitions. Therefore, in a given region of relevance where a particular phase variable is locked, the properties of the resulting phase that may exhibit dominant QLRO can be understood by analyzing the exponents of the order-parameter correlations.

For this purpose, the analysis based on the RG equations given by Eqs. (4.4) is not simple since the G_{3p} term contains both ϕ_s and θ_s ($s = f, \psi$) fields. When treating this type of term, one often encounters subtleties in determining ground-state phases, especially in the case that the G_{3p} term becomes relevant. Thus it is necessary to make transformation to a suitable basis.

A. Recombination of phase variables

We perform the following canonical transformation:

$$\boldsymbol{\varphi}(x) = P\,\boldsymbol{\phi}(x), \quad \boldsymbol{\vartheta}(x) = Q\,\boldsymbol{\theta}(x), \tag{5.1}$$

where

$$\boldsymbol{\phi}(x) = \begin{pmatrix} \phi_b(x) \\ \phi_f(x) \\ \phi_\psi(x) \end{pmatrix}, \quad \boldsymbol{\theta}(x) = \begin{pmatrix} \theta_b(x) \\ \theta_f(x) \\ \theta_\psi(x) \end{pmatrix}, \tag{5.2a}$$

$$\boldsymbol{\varphi}(x) = \begin{pmatrix} \varphi_1(x) \\ \varphi_2(x) \\ \varphi_3(x) \end{pmatrix}, \quad \boldsymbol{\vartheta}(x) = \begin{pmatrix} \vartheta_1(x) \\ \vartheta_2(x) \\ \vartheta_3(x) \end{pmatrix}. \tag{5.2b}$$

The transformation matrices P and Q are generally nonorthogonal, but the commutation relations of φ and ϑ, $[\varphi_a(x), \pi^{-1}\partial_y \vartheta_b(y)] = i\delta_{a,b}\delta(x-y)$, are preserved as long as the relation $PQ^{\mathrm{T}} = 1$ is satisfied [42]. A simplification of Eq. (3.4) follows from the following choice of the matrices:

$$P = \frac{1}{\sqrt{2}}\begin{pmatrix} -2 & 1 & -1 \\ 0 & 1 & 1 \\ 0 & 1 & -1 \end{pmatrix}, \quad Q = \frac{1}{\sqrt{2}}\begin{pmatrix} -1 & 0 & 0 \\ 0 & 1 & 1 \\ 1 & 1 & -1 \end{pmatrix}. \tag{5.3}$$

Substituting the phase variables $\boldsymbol{\varphi}$ and $\boldsymbol{\vartheta}$, we rewrite the cosine terms in Eqs. (4.1) as

$$S_{I,1} = \frac{G_{3p}}{i\pi}\int \frac{d^2r}{\alpha^2}\cos(\sqrt{2}\vartheta_3)\sin(\sqrt{2}\varphi_3), \tag{5.4a}$$

$$S_{I,2} = \frac{G_\phi}{\pi}\int \frac{d^2r}{\alpha^2}\cos(2\sqrt{2}\varphi_3), \tag{5.4b}$$

$$S_{I,3} = \frac{G_\theta}{\pi}\int \frac{d^2r}{\alpha^2}\cos(2\sqrt{2}\vartheta_3). \tag{5.4c}$$

We note that the phase variables φ_3 and ϑ_3 are under the influence of the G_ϕ and G_θ cosine potentials, respectively. In terms of the phase variables $\boldsymbol{\varphi}$ and $\boldsymbol{\vartheta}$, the TLL Hamiltonian (3.3) is rewritten as

$$\begin{aligned} H_0 &= H_b + H_f + H_\psi \\ &= \frac{1}{2\pi}\int dx[(\partial_x\boldsymbol{\varphi}^{\mathrm{T}})M(\partial_x\boldsymbol{\varphi}) + (\partial_x\boldsymbol{\vartheta}^{\mathrm{T}})N(\partial_x\boldsymbol{\vartheta})], \end{aligned} \tag{5.5}$$

where M and N are real symmetric matrices defined by

$$M = \frac{1}{2}\begin{pmatrix} u_b K_b^{-1} & 0 & -u_b K_b^{-1} \\ 0 & u_f K_f^{-1} + u_\psi K_\psi^{-1} & u_f K_f^{-1} - u_\psi K_\psi^{-1} \\ -u_b K_b^{-1} & u_f K_f^{-1} - u_\psi K_\psi^{-1} & u_b K_b^{-1} + u_f K_f^{-1} + u_\psi K_\psi^{-1} \end{pmatrix}, \tag{5.6a}$$

$$N = \frac{1}{2}\begin{pmatrix} 4u_b K_b + u_f K_f + u_\psi K_\psi & u_f K_f - u_\psi K_\psi & u_f K_f + u_\psi K_\psi \\ u_f K_f - u_\psi K_\psi & u_f K_f + u_\psi K_\psi & u_f K_f - u_\psi K_\psi \\ u_f K_f + u_\psi K_\psi & u_f K_f - u_\psi K_\psi & u_f K_f + u_\psi K_\psi \end{pmatrix}. \tag{5.6b}$$

The order parameters introduced in Sec. III B can now be expressed in terms of the new phase variables $\boldsymbol{\varphi}$ and $\boldsymbol{\vartheta}$. The order parameters for the b particles are given by

$$\mathcal{O}_b^{\mathrm{SF}}(x) \simeq e^{-i\sqrt{2}\vartheta_1}, \tag{5.7a}$$

$$\mathcal{O}_b^{\mathrm{DW}}(x) \simeq e^{i2k_F^b x + i\sqrt{2}\varphi_1 - i\sqrt{2}\varphi_3}. \tag{5.7b}$$

The order parameters for the p-wave-pairing SF and out-of-phase DW states of the f and ψ particles are written as

$$\mathcal{O}_{f\psi}^{\mathrm{SF}}(x) \simeq e^{i\sqrt{2}\vartheta_2}\sin(\sqrt{2}\varphi_3), \tag{5.7c}$$

$$\mathcal{O}_{f\psi}^{\mathrm{DW}}(x) \simeq e^{i2k_F x - i\sqrt{2}\varphi_2}\sin(\sqrt{2}\varphi_3), \tag{5.7d}$$

from which it follows that correlations of $\mathrm{SF}_{f\psi}$ and $\mathrm{DW}_{f\psi}$ are enhanced when the phase field φ_3 is locked at $\langle\sqrt{2}\varphi_3\rangle = \pi/2 \mod \pi$. Finally, the order parameters for the composite particles are expressed as

$$\mathcal{O}_{bff+b^\dagger\psi\psi}^{\mathrm{SF}}(x) \simeq e^{i\sqrt{2}\vartheta_2}\cos(\sqrt{2}\vartheta_3), \tag{5.7e}$$

$$\mathcal{O}_{b^\dagger f^\dagger\psi}^{\mathrm{ph1}}(x) \simeq e^{-i\sqrt{2}\varphi_3}\sin(\sqrt{2}\vartheta_3) + e^{-i2k_F^b x - i\sqrt{2}\varphi_1}\cos(\sqrt{2}\vartheta_3), \tag{5.7f}$$

$$\mathcal{O}_{b^\dagger f^\dagger\psi}^{\mathrm{ph2}}(x) \simeq e^{i2k_F x - i\sqrt{2}\varphi_2}\cos(\sqrt{2}\vartheta_3). \tag{5.7g}$$

We see that the correlations of these order parameters are enhanced when the phase field ϑ_3 is locked at $\langle\sqrt{2}\vartheta_3\rangle = 0 \mod \pi$, except for the first contribution in Eq. (5.7f).

B. Effective low-energy Hamiltonian

The sinusoidal potentials of Eqs. (5.4) take on forms similar to those of the spinless two-coupled chain system [35,37] (see Appendix A). In the two-chain system, operators generated in RG transformations become relevant in the low-energy limit. Similarly, we expect that either the G_ϕ or G_θ term can become relevant and renormalized to strong coupling, as we have discussed below Eq. (4.8). The relevant $G_\phi > 0$ leads to locking of the phase field φ_3 at $\langle\sqrt{2}\varphi_3\rangle = \pi/2 \mod \pi$, whereas the relevant $G_\theta < 0$ leads to the locking of the phase field ϑ_3 at $\langle\sqrt{2}\vartheta_3\rangle = 0 \mod \pi$. When either φ_3 or ϑ_3 is locked, the remaining phase fields φ_s and ϑ_s ($s = 1,2$) remain gapless, and then the system is effectively described by a two-component TLL and a massive sine-Gordon model. However, in contrast to the simple forms of sinusoidal potentials, the quadratic Hamiltonian in Eq. (5.5) is complicated by the presence of many cross terms. One approach that we will implement here is to integrate out the massive mode (φ_3, ϑ_3) in a manner similar to Ref. [43], thereby reducing the problem to a two-band system which can be exactly diagonalized. To be more precise, when $G_\phi(l) \to +\infty$ in the RG analysis, the quantum fluctuations of the φ_3 field are suppressed, and we can make the approximation $\partial_x\varphi_3 \to \partial_x\langle\varphi_3\rangle \sim 0$. Moreover, since the cosine potentials can be ignored for the strongly fluctuating ϑ_3 field, ϑ_3 can be integrated out by completing the square for $\partial_x\vartheta_3$ in the quadratic Hamiltonian, as described in Ref. [43]. The same approach can be used for $G_\theta(l) \to -\infty$. Consequently, the system can be described effectively by the two-component TL liquid with the effective low-energy Hamiltonian

$$H^{\mathrm{eff}} = \sum_{i,j=1,2}\int \frac{dx}{2\pi}(\bar{M}_{ij}\varphi_i'\varphi_j' + \bar{N}_{ij}\vartheta_i'\vartheta_j'), \tag{5.8}$$

where $\varphi_i' = \partial_x\varphi_i$ and $\vartheta_i' = \partial_x\vartheta_i$. In the case when φ_3 is locked ($G_\phi \to \infty$), the renormalized coefficients are given by $\bar{M}_{ij} = M_{ij}$ and $\bar{N}_{ij} = N_{ij} - N_{i3}N_{j3}/N_{33}$ $(i,j = 1,2)$. Similarly, when ϑ_3 is locked ($G_\theta \to -\infty$), the coefficients are given by $\bar{M}_{ij} = M_{ij} - M_{i3}M_{j3}/M_{33}$ and $\bar{N}_{ij} = N_{ij}$.

The Hamiltonian (5.8) can be diagonalized sequentially [42], yielding

$$H^{\mathrm{eff}} = \frac{u_1}{2\pi}\int dx[(\partial_x\tilde{\varphi}_1)^2 + (\partial_x\tilde{\vartheta}_1)^2] + \frac{u_2}{2\pi}\int dx[(\partial_x\tilde{\varphi}_2)^2 + (\partial_x\tilde{\vartheta}_2)^2]. \tag{5.9}$$

The canonical transformation between the phase variables (φ, ϑ) and $(\tilde{\varphi}, \tilde{\vartheta})$ are given by

$$\begin{pmatrix}\varphi_1 \\ \varphi_2\end{pmatrix} = \bar{P}\begin{pmatrix}\tilde{\varphi}_1 \\ \tilde{\varphi}_2\end{pmatrix}, \quad \begin{pmatrix}\vartheta_1 \\ \vartheta_2\end{pmatrix} = \bar{Q}\begin{pmatrix}\tilde{\vartheta}_1 \\ \tilde{\vartheta}_2\end{pmatrix}, \tag{5.10}$$

where the transformation matrices $\bar{P}$ and $\bar{Q}$ are defined as $\bar{P} = R_1\Delta_1^{-1/2}R_2\Delta_2^{1/4}$ and $\bar{Q} = R_1\Delta_1^{1/2}R_2\Delta_2^{-1/4}$ with Δ_1 and Δ_2 being diagonal matrices. Here the rotation matrix R_1 diagonalizes the matrix $\bar{M}$ as $R_1^{\mathrm{T}}\bar{M}R_1 = \Delta_1$, and the rotation matrix R_2 diagonalizes the matrix $\Delta_1^{1/2}R_1^{\mathrm{T}}\bar{N}R_1\Delta_1^{1/2} = R_2\Delta_2R_2^{\mathrm{T}}$. The velocities u_1 and u_2 are diagonal elements of $\Delta_2^{1/2}$.

C. Correlation exponents

In this section we calculate correlation exponents for order parameters characterizing the phases in Fig. 3(b).

For the Gaussian model (5.9), the correlation functions of vertex operators, $\exp(i\lambda_i\varphi_i)$ and $\exp(i\lambda_i\vartheta_i)$ with real parameters $\lambda_{1,2}$, show power-law decay,

$$\langle e^{i\lambda_1\varphi_1(x)+i\lambda_2\varphi_2(x)}e^{-i\lambda_1\varphi_1(0)-i\lambda_2\varphi_2(0)}\rangle \sim x^{-\frac{1}{2}\lambda_1^2\eta_{\varphi 1}-\frac{1}{2}\lambda_2^2\eta_{\varphi 2}-\lambda_1\lambda_2\eta_{\varphi 12}}, \tag{5.11a}$$

$$\langle e^{i\lambda_1\vartheta_1(x)+i\lambda_2\vartheta_2(x)}e^{-i\lambda_1\vartheta_1(0)-i\lambda_2\vartheta_2(0)}\rangle \sim x^{-\frac{1}{2}\lambda_1^2\eta_{\vartheta 1}-\frac{1}{2}\lambda_2^2\eta_{\vartheta 2}-\lambda_1\lambda_2\eta_{\vartheta 12}}, \tag{5.11b}$$

where the exponents are given by

$$\eta_{\varphi i} = \sum_{j=1,2} \bar{P}_{ij}^2, \quad \eta_{\varphi 12} = \sum_{j=1,2} \bar{P}_{1j}\bar{P}_{2j}, \tag{5.12a}$$

$$\eta_{\vartheta i} = \sum_{j=1,2} \bar{Q}_{ij}^2, \quad \eta_{\vartheta 12} = \sum_{j=1,2} \bar{Q}_{1j}\bar{Q}_{2j}. \tag{5.12b}$$

These results can be applied to the cases of interest.

1. Case of relevant G_ϕ

In the case when G_ϕ is renormalized to strong coupling ($G_\phi \to \infty$), the fluctuations in the ϑ_3 field diverge, and, consequently, the order parameters that contain the vertex operator of ϑ_3 exhibit short-range correlations or exponential decay at large distances. On the other hand, the locked field φ_3 can be replaced by its average $\langle\sqrt{2}\varphi_3\rangle = \pi/2 \mod \pi$ in the order parameters that contain φ_3. The correlation functions for the boson order parameters are then given by

$$\left\langle \mathcal{O}_b^{\mathrm{SF}}(x)\,\mathcal{O}_b^{\mathrm{SF}\dagger}(0)\right\rangle \sim x^{-1/(2K_b)}, \tag{5.13a}$$

$$\left\langle \mathcal{O}_b^{\mathrm{DW}}(x)\,\mathcal{O}_b^{\mathrm{DW}\dagger}(0)\right\rangle \sim x^{-2K_b}e^{i2k_F^b x}. \tag{5.13b}$$

We note that the exponents are unchanged from those in the $g_{3p} = 0$ case [see Eqs. (3.6)] and that the correlation functions of b particles are controlled by the TLL parameter K_b. (To be precise, K_b should be replaced by its renormalized value K_b^*, whose difference from K_b is on the order of g_{3p}^4.) The SF_b is dominant for $K_b > 1/2$, while the DW_b becomes dominant for $K_b < 1/2$. For f and ψ particles, slowly decaying correlation functions are given by

$$\left\langle \mathcal{O}_{f\psi}^{\mathrm{SF}}(x)\,\mathcal{O}_{f\psi}^{\mathrm{SF}\dagger}(0)\right\rangle \sim x^{-1/K_2}, \tag{5.14a}$$

$$\left\langle \mathcal{O}_{f\psi}^{\mathrm{DW}}(x)\,\mathcal{O}_{f\psi}^{\mathrm{DW}\dagger}(0)\right\rangle \sim x^{-K_2}e^{i2k_F x}, \tag{5.14b}$$

where

$$K_2 = 2\left[\left(\frac{u_f}{K_f}+\frac{u_\psi}{K_\psi}\right)\left(\frac{1}{u_f K_f}+\frac{1}{u_\psi K_\psi}\right)\right]^{-1/2}. \tag{5.14c}$$

The most dominant order for f and ψ particles is determined by K_2: The $\mathrm{SF}_{f\psi}$ state for $K_2 > 1$ and the $\mathrm{DW}_{f\psi}$ state for $K_2 < 1$. In the phase diagram shown in Fig. 3(b), the region of relevant G_ϕ is classified into four regions according to the most slowly decaying correlation for the bosonic (b) and fermionic (f, ψ) particles.

Here we briefly discuss the correspondence to the results obtained in Ref. [18], in which the f-ψ paired state is predicted within a mean-field analysis of a 3D model. It is pointed out in Ref. [18] that the molecular conversion term induces a *repulsive* density-density interaction between a fermionic atom and a molecule through a lowest-order virtual process. This effective interaction is consistent with the interaction vertex $G_\phi > 0$ generated in our perturbative RG analysis. Furthermore, it is argued in Ref. [18] that, if the bosons are *condensed*, the effective interaction between a fermionic atom and a molecule can become *attractive*, thereby yielding the SF order of "s-wave" f-ψ pairing state. In the present 1D case, the mean-field theory is invalid (bosons cannot condense), and the effective interaction G_ϕ is repulsive. Therefore the s-wave f-ψ pairing cannot be stabilized. Instead, we obtain a "p-wave" f-ψ pairing (or out-of-phase DW state of f and ψ particle) which can be stabilized due to the induced *repulsive* interaction between f and ψ particles.

2. Case of relevant G_θ

Next we consider the case where the phase field ϑ_3 is locked. The fluctuations of the φ_3 field are divergent, and its order parameters exhibit short-range correlations. The order parameters of our interest are those involving ϑ_3, which can be simplified by replacing $\sqrt{2}\vartheta_3$ with its expectation value $\langle\sqrt{2}\vartheta_3\rangle = 0 \mod \pi$. The correlation functions of these leading order parameters exhibit algebraic decay,

$$\left\langle \mathcal{O}_b^{\mathrm{SF}}(x)\,\mathcal{O}_b^{\mathrm{SF}\dagger}(0)\right\rangle \sim x^{-\eta_{\vartheta 1}}, \tag{5.15a}$$

$$\left\langle \mathcal{O}_{bff+b^\dagger\psi\psi}^{\mathrm{SF}}(x)\,\mathcal{O}_{bff+b^\dagger\psi\psi}^{\mathrm{SF}\dagger}(0)\right\rangle \sim x^{-\eta_{\vartheta 2}}, \tag{5.15b}$$

$$\left\langle \mathcal{O}_{b^\dagger f^\dagger\psi}^{\mathrm{ph1}}(x)\,\mathcal{O}_{b^\dagger f^\dagger\psi}^{\mathrm{ph1}\dagger}(0)\right\rangle \sim x^{-\eta_{\varphi 1}}e^{-i2k_F^b x}, \tag{5.15c}$$

$$\left\langle \mathcal{O}_{b^\dagger f^\dagger\psi}^{\mathrm{ph2}}(x)\,\mathcal{O}_{b^\dagger f^\dagger\psi}^{\mathrm{ph2}\dagger}(0)\right\rangle \sim x^{-\eta_{\varphi 2}}e^{i2k_F x}. \tag{5.15d}$$

The correlation functions of the order parameters $\mathcal{O}_{ff}^{\mathrm{SF}}(x)$ and $\mathcal{O}_{\psi\psi}^{\mathrm{SF}}(x)$ also exhibit algebraic decay. However, these orders cannot dominate over those given in Eqs. (5.15), since their exponents are always greater than those in Eqs. (5.15).

When $u_b = u_f = u_\psi$ and $K_f = K_\psi$, the Hamiltonian (5.8) takes a diagonal form, and the exponents are simplified to

$$\eta_{\varphi 1} = 2K_b + K_f, \quad \eta_{\varphi 2} = K_f, \tag{5.16a}$$

$$\eta_{\vartheta 1} = \frac{1}{2K_b + K_f}, \quad \eta_{\vartheta 2} = \frac{1}{K_f}. \tag{5.16b}$$

In the parameter region in Fig. 3(b) where G_θ flows to strong coupling, the exponent $\eta_{\vartheta 1}$ is always smaller than the others in Eqs. (5.16). Hence, the SF_b state is designated as the most dominant state. We also note that the SF_b correlation is enhanced as compared with the case of $g_{3p} = 0$ where $\eta_{\vartheta 1} \to 1/(2K_b)$.

VI. DISCUSSION AND CONCLUDING REMARKS

In summary, we have carried out a comprehensive study of a two-channel Bose-Fermi mixture, for which the analysis and results presented here can possibly be applied towards more general many-body problems involving interacting multicomponent quantum liquids.

When the densities of the fermionic atoms and fermionic MB molecules are identical, the Feshbach molecule conversion and disassociation, the g_{3p} term, can become relevant and

induce an excitation gap, while the system retains two gapless modes. One appealing feature of the phase diagram in particular is the existence of a dominant composite p-wave pairing state $\Psi_f^L \Psi_\psi^R$, which occurs for fermions in both the open and closed hyperfine channels, induced by an effective interaction mediated by b atoms. Ultimately, we hope that the phase diagram presented here should demonstrate more general features of composite orders and indirect scattering processes that will manifest in higher dimensions.

Although we have established the qualitative behavior of the phase diagram for a wide range of interaction couplings, a better comparison with experiments will require microscopic determination of the TLL parameters using numerical methods. Since our model contains specific order parameters that couple different atomic species, a direct experimental probe must be sensitive to interspecies density correlations. Time-of-flight spectroscopy is the most promising method, as it can directly image an atomic cloud's density profile, which should demonstrate specific commensurability in the presence of density wavelike order [6]. A possible experimental realization within the cold atoms systems would involve a magnetic trapping technique developed on atom chips [44]. Recently, the TLL signatures have been confirmed by observing certain quasi-long-range order within the noise correlations between two independent 1D bosonic atomic condensates created on an atom chip [45]. As discussed in Ref. [46], the analysis of the noise correlations would be also useful to detect the composite pairing states proposed in the present paper, since this measurement would be sensitive not only to density-wave fluctuations but also to pairing fluctuations.

In order to make a proper comparison of the results obtained in this paper with actual experiments in trapped cold atom systems, we have to take into account the density inhomogeneity arising from the harmonic trap. For this purpose, we can apply the local density approximation (LDA) [47] when the range of the density variation is much larger than the average interparticle distance. In the incommensurate case ($\bar{\rho}_f \neq \bar{\rho}_\psi$), where the system is described as the three-component TLL in the homogeneous limit, the low-energy properties can be analyzed by the bosonization scheme based on the LDA [23,48]. On the other hand, in the commensurate case ($\bar{\rho}_f = \bar{\rho}_\psi$), the extension of the RG analysis would not be so straightforward. The numerical studies on the trapped boson system in an optical lattice [49,50] have shown the transition from a superfluid to a Mott insulating state in the so-called "wedding cake" structure with density plateaus of the Mott state, which was indeed observed experimentally [51]. Such a structure can be ascribed to the commensurability effect which is present when the number of bosons per site becomes integer. Since the commensurability effects can be represented as the sinusoidal potentials in the bosonization scheme, we expect that similar commensurate-incommensurate transitions should be realized when a trapping potential is taken into account in the present system.

ACKNOWLEDGMENTS

We thank T. Giamarchi, E. Orignac, and Masahiro Sato for important discussions. S.A. acknowledges helpful conversations with A. M. Tsvelik and support from the RIKEN FPR program.

APPENDIX A: TWO-COUPLED CHAIN REVISITED

The model which we consider in the present paper has a close connection to the model of spinless two chains coupled by the one-particle interchain hopping [35,38]. The model Hamiltonian for the two-coupled chains is given by

$$\begin{aligned} H_{2\,\mathrm{chain}} = & \sum_{s=1,2} \int dx\, iv \left(\Psi_s^{L\dagger} \partial_x \Psi_s^L - \Psi_s^{R\dagger} \partial_x \Psi_s^R \right) \\ & - t_\perp \sum_{p=L,R} \int dx \left(\Psi_1^{p\dagger} \Psi_2^p + \mathrm{H.c.} \right) \\ & + \int dx \, [g(\rho_1 \rho_1 + \rho_2 \rho_2) + 2g' \rho_1 \rho_2], \end{aligned} \tag{A1}$$

where $p = L\,(R)$ refers to the left-(right-) moving particle and $s = 1,2$ is the chain index. The couplings g and g' represent the intrachain and interchain interactions, respectively [35]. In earlier works, the interchain hopping term is diagonalized by introducing the bonding and antibonding band basis of the field operators, and then the bosonization and RG methods are applied to the field operators on the band basis [35,38]. In this appendix, we verify that the same results can be obtained by directly applying the bosonization to the field operators on the original chain basis. The bosonized forms of the field operators are given by

$$\Psi_s^{L/R}(x) = \frac{\xi_s}{\sqrt{2\pi\alpha}} e^{\mp i k_F x \pm i\phi_s(x) + i\theta_s(x)}, \tag{A2}$$

where $s = 1,2$ is the chain index and ξ_s is the Klein factor satisfying $\xi_1 \xi_2 = i$. The commutation relation of the phase variables is $[\phi_s(x), \theta_{s'}(x')] = i\pi \delta_{s,s'} \Theta(-x + x')$. Since a dominant phase can be determined by the locking position of ϕ_s or θ_s, we have to carefully apply the fusion rules for vertex operators.

With the symmetric and antisymmetric combinations of phase variables, $\phi_\pm = (\phi_1 \pm \phi_2)/\sqrt{2}$ and $\theta_\pm = (\theta_1 \pm \theta_2)/\sqrt{2}$, the bosonized Hamiltonian is written as

$$\begin{aligned} H_{2\,\mathrm{chain}} = & \frac{u_+}{2\pi} \int dx \left[\frac{1}{K_+} (\partial_x \phi_+)^2 + K_+ (\partial_x \theta_+)^2 \right] \\ & + \frac{u_-}{2\pi} \int dx \left[\frac{1}{K_-} (\partial_x \phi_-)^2 + K_- (\partial_x \theta_-)^2 \right] \\ & + i \frac{u_- G_\perp}{\pi \alpha^2} \int dx \cos\sqrt{2}\theta_- \sin\sqrt{2}\phi_- \\ & + \frac{u_- \widetilde{G}_\phi}{\pi \alpha^2} \int dx \cos 2\sqrt{2}\phi_- \\ & + \frac{u_- \widetilde{G}_\theta}{\pi \alpha^2} \int dx \cos 2\sqrt{2}\theta_-, \end{aligned} \tag{A3}$$

where $K_\pm \simeq 1 - (g \pm g')/(\pi v)$, $u_\pm \simeq v + (g \pm g')/\pi$, and $G_\perp = 2t_\perp \alpha / u_-$. The coupling constants $\widetilde{G}_\phi$ and $\widetilde{G}_\theta$ are initially zero but generated through the RG transformation. Only the asymmetric fields (ϕ_-, θ_-) are subject to the sinusoidal potentials, and the symmetric fields (ϕ_+, θ_+) remain free.

The order parameters characterizing the ground state are written in the bosonized form as [35,38]

$$O_{\mathrm{CDW}^\pi}(x) = \Psi_1^{L\dagger}\Psi_1^R - \Psi_2^{L\dagger}\Psi_2^R \simeq e^{i2k_F x - i\sqrt{2}\phi_+}\sin\sqrt{2}\phi_-, \tag{A4a}$$

$$O_{\mathrm{OAF}}(x) = \Psi_1^{L\dagger}\Psi_2^R - \Psi_2^{L\dagger}\Psi_1^R \simeq e^{i2k_F x - i\sqrt{2}\phi_+}\cos\sqrt{2}\theta_-, \tag{A4b}$$

$$O_{\mathrm{SC}^d}(x) = \Psi_1^L\Psi_2^R + \Psi_2^L\Psi_1^R \simeq e^{i\sqrt{2}\theta_+}\sin\sqrt{2}\phi_-, \tag{A4c}$$

$$O_{\mathrm{SC}^s}(x) = \Psi_1^L\Psi_1^R + \Psi_2^L\Psi_2^R \simeq e^{i\sqrt{2}\theta_+}\cos\sqrt{2}\theta_-, \tag{A4d}$$

where CDW$^\pi$, OAF, SC^d, and SC^s stand for charge-density wave, orbital antiferromagnetic, d-wave superconducting, and s-wave superconducting states, respectively.

In order to analyze the low-energy behavior of the ϕ_- mode, we apply the momentum-shell renormalization-group method [33]. First, we split the phase variable as $\phi_s = \phi_s' + h_s$ and $\theta_s = \theta_s' + \tilde{h}_s$, where ϕ_s' and h_s are the phase fields containing low-momentum and high-momentum components, respectively,

$$\phi_s'(\boldsymbol{r}) = \int_{|k|\lesssim\Lambda'} \frac{d^2k}{(2\pi)^2}\, e^{i\boldsymbol{k}\cdot\boldsymbol{r}}\,\phi_s(\boldsymbol{k}), \tag{A5a}$$

$$h_s(\boldsymbol{r}) = \int_{\Lambda'\lesssim|k|\lesssim\Lambda} \frac{d^2k}{(2\pi)^2}\, e^{i\boldsymbol{k}\cdot\boldsymbol{r}}\,\phi_s(\boldsymbol{k}), \tag{A5b}$$

where $\boldsymbol{r} = (x,u_s\tau)$, $\boldsymbol{k} = (k,\omega/u_s)$, $\boldsymbol{k}\cdot\boldsymbol{r} = kx - \omega\tau$ [33], and $\phi_s(\boldsymbol{k})$ is the Fourier transform of $\phi_s(x,\tau)$. The fields θ_s' and $\tilde{h}_s$ are defined similarly as low- and high-momentum components of the conjugate fields θ_s. The RG equations are derived by integrating out the h and $\tilde{h}$ fields with the help of Eq. (4.3).

We perform RG transformations of the action S by treating the interchain hopping part,

$$S_\perp = i\frac{G_\perp}{\pi}\int \frac{d^2r}{\alpha^2}\,\cos\sqrt{2}\theta_-(\boldsymbol{r})\,\sin\sqrt{2}\phi_-(\boldsymbol{r}), \tag{A6}$$

as a weak perturbation, where $d^2r = u_-dxd\tau$. In doing so, we have to pay special attention to the commutative properties. The equal-time commutation relation between ϕ_s and θ_s is given by

$$[\phi_s(x),\theta_{s'}(x')] = i\pi\delta_{s,s'}\Theta(-x+x'), \tag{A7}$$

and their correlation functions are given by [33]

$$\langle\phi_s(\boldsymbol{r})\theta_s(0)\rangle = \frac{1}{2}F_2(\boldsymbol{r}) + \frac{i\pi}{4}, \tag{A8a}$$

$$\langle\theta_s(\boldsymbol{r})\phi_s(0)\rangle = \frac{1}{2}F_2(\boldsymbol{r}) - \frac{i\pi}{4}, \tag{A8b}$$

where $F_2(\boldsymbol{r}) = -i\,\mathrm{Arg}(y_\alpha + ix)$ with $y_\alpha = u_s\tau + \alpha\,\mathrm{sgn}(\tau)$. The last terms $\pm i\pi/4$ in Eqs. (A8) are added in order to reproduce the commutation relation (A7). Integrating out the h_s fields yields the $O(t_\perp^2)$ contribution to the action S,

$$\begin{aligned}-\frac{1}{2}\langle S_\perp^2\rangle_h^c = &-\frac{G_\perp^2}{32\pi^2}\sum_{\epsilon,\epsilon'=\pm}\int\frac{d^2r_1}{\alpha^2}\frac{d^2r_2}{\alpha^2}\\ &\times\langle e^{i\epsilon\sqrt{2}\theta_-(1)}e^{i\epsilon'\sqrt{2}\phi_-(1)}e^{-i\epsilon\sqrt{2}\theta_-(2)}e^{i\epsilon'\sqrt{2}\phi_-(2)}\rangle_h^c\\ &+\frac{G_\perp^2}{32\pi^2}\sum_{\epsilon,\epsilon'=\pm}\int\frac{d^2r_1}{\alpha^2}\frac{d^2r_2}{\alpha^2}\\ &\times\langle e^{i\epsilon\sqrt{2}\theta_-(1)}e^{i\epsilon'\sqrt{2}\phi_-(1)}e^{i\epsilon\sqrt{2}\theta_-(2)}e^{-i\epsilon'\sqrt{2}\phi_-(2)}\rangle_h^c,\end{aligned} \tag{A9}$$

where (1) and (2) stand for $(\boldsymbol{r}_1)$ and $(\boldsymbol{r}_2)$, respectively, and $\langle\cdots\rangle_h^c$ is the cumulant expectation with respect to the h and $\tilde{h}$ fields. The cumulant expectations can be evaluated as

$$\begin{aligned}&\langle e^{i\epsilon\sqrt{2}\theta_-(1)}e^{i\epsilon'\sqrt{2}\phi_-(1)}e^{-i\epsilon\sqrt{2}\theta_-(2)}e^{i\epsilon'\sqrt{2}\phi_-(2)}\rangle_h^c\\ &\quad= e^{i\epsilon\sqrt{2}\theta_-'(1)}e^{i\epsilon'\sqrt{2}\phi_-'(1)}e^{-i\epsilon\sqrt{2}\theta_-'(2)}e^{i\epsilon'\sqrt{2}\phi_-'(2)}\\ &\qquad\times e^{-(K_-+K_-^{-1})\delta g(\boldsymbol{0})}\left[e^{(K_-^{-1}-K_-)\delta g(r_{12})}-1\right].\end{aligned} \tag{A10}$$

We note that the integrand becomes nonzero only for small $r_{12}/\alpha = |\boldsymbol{r}_1 - \boldsymbol{r}_2|/\alpha$ since the function $\delta g(r)$ decays rapidly in r/α. We can rewrite the product of the vertex operators as

$$\begin{aligned}&e^{i\epsilon\sqrt{2}\theta_-'(1)}e^{i\epsilon'\sqrt{2}\phi_-'(1)}e^{-i\epsilon\sqrt{2}\theta_-'(2)}e^{i\epsilon'\sqrt{2}\phi_-'(2)}\\ &\quad\approx -e^{i\epsilon\sqrt{2}\theta_-'(1)+i\epsilon'\sqrt{2}\phi_-'(1)-i\epsilon\sqrt{2}\theta_-'(2)+i\epsilon'\sqrt{2}\phi_-'(2)},\end{aligned} \tag{A11}$$

where we have used $[\phi_s'(\boldsymbol{r}_1),\theta_s'(\boldsymbol{r}_2)] + [\phi_s'(\boldsymbol{r}_2),\theta_s'(\boldsymbol{r}_1)] = \langle[\phi_s'(\boldsymbol{r}_1),\theta_s'(\boldsymbol{r}_2)]\rangle + \langle[\phi_s'(\boldsymbol{r}_2),\theta_s'(\boldsymbol{r}_1)]\rangle = i\pi$, together with the relation (A8). Using Eq. (4.6), we can perform the operator-product expansion [$r_{12} = |\boldsymbol{r}_1 - \boldsymbol{r}_2|$ and $\boldsymbol{R} = (\boldsymbol{r}_1 + \boldsymbol{r}_2)/2$]:

$$\begin{aligned}&e^{i\epsilon\sqrt{2}\theta_-'(1)+i\epsilon'\sqrt{2}\phi_-'(1)-i\epsilon\sqrt{2}\theta_-'(2)+i\epsilon'\sqrt{2}\phi_-'(2)}\\ &\quad\approx :e^{i\epsilon\sqrt{2}\theta_-'(1)+i\epsilon'\sqrt{2}\phi_-'(1)-i\epsilon\sqrt{2}\theta_-'(2)+i\epsilon'\sqrt{2}\phi_-'(2)}:\\ &\qquad\times e^{-K_-^{-1}[\bar{g}(0)-\bar{g}(r_{12})]}e^{-K_-[\bar{g}(0)+\bar{g}(r_{12})]}\\ &\quad\approx :e^{+i\epsilon'2\sqrt{2}\phi_-'(\boldsymbol{R})}:\ e^{-K_-^{-1}[\bar{g}(0)-\bar{g}(r_{12})]}e^{-K_-[\bar{g}(0)+\bar{g}(r_{12})]}\\ &\quad= e^{+i\epsilon'2\sqrt{2}\phi_-'(\boldsymbol{R})}e^{-(K_-^{-1}-K_-)[\bar{g}(0)-\bar{g}(r_{12})]},\end{aligned} \tag{A12}$$

where $\bar{g}(r)$ is given in Eq. (4.2), and we have used Eqs. (A8). Thus we find

$$\begin{aligned}-\frac{1}{2}\langle S_\perp^2\rangle_h^c = &+\frac{G_\perp^2}{4\pi}e^{-(K_-+K_-^{-1})\delta g(\boldsymbol{0})}A_1((K_-^{-1}-K_-)/2)\,dl\\ &\times\int\frac{d^2R}{\alpha^2}\cos 2\sqrt{2}\phi_-'(\boldsymbol{R})\\ &-\frac{G_\perp^2}{4\pi}e^{-(K_-+K_-^{-1})\delta g(\boldsymbol{0})}A_1((K_--K_-^{-1})/2)\,dl\\ &\times\int\frac{d^2R}{\alpha^2}\cos 2\sqrt{2}\theta_-'(\boldsymbol{R}),\end{aligned} \tag{A13}$$

where $A_i(\beta)$ is defined in Eqs. (4.5). The first (second) term renormalizes the $\tilde{G}_\phi$ ($\tilde{G}_\theta$) term. The full RG equations for the

coupling constants and the TLL parameter K_- are given by

$$\frac{dG_\perp}{dl} = \left(2 - \frac{K_-}{2} - \frac{1}{2K_-}\right) G_\perp, \tag{A14a}$$

$$\frac{d\widetilde{G}_\phi}{dl} = (2 - 2K_-)\widetilde{G}_\phi + \frac{1}{4}G_\perp^2 A_1((K_-^{-1} - K_-)/2), \tag{A14b}$$

$$\frac{d\widetilde{G}_\theta}{dl} = (2 - 2K_-^{-1})\widetilde{G}_\theta - \frac{1}{4}G_\perp^2 A_1((K_- - K_-^{-1})/2), \tag{A14c}$$

$$\frac{dK_-}{dl} = -2\widetilde{G}_\phi^2 K_-^2 A_2(2K_-) + 2\widetilde{G}_\theta^2 A_2(2K_-^{-1}). \tag{A14d}$$

We see from Eqs. (A14b) and (A14c) that the one-loop RG processes yield contributions of order $G_\perp^2$ to $\widetilde{G}_\phi$ and $\widetilde{G}_\theta$, respectively. Consequently, when $K_- < 1$, the coupling $\widetilde{G}_\phi$ is relevant and renormalized to strong coupling ($\widetilde{G}_\phi \to +\infty$). In this case, the phase field ϕ_- is locked at $\langle\sqrt{2}\phi_-\rangle = \pi/2$ mod π. On the other hand, if $K_- > 1$, the coupling $\widetilde{G}_\theta$ is relevant and renormalized to strong coupling ($\widetilde{G}_\theta \to -\infty$), and then the phase field θ_- is locked at $\langle\sqrt{2}\theta_-\rangle = 0 \mod \pi$.

For $K_- < 1$ (i.e., $g > g'$), the relevant order parameters, CDW$^\pi$ and SC^d, are reduced to $O_{\mathrm{CDW}^\pi}(x) \to e^{i2k_F x - i\sqrt{2}\phi_+}$, $O_{\mathrm{SC}^d}(x) \to e^{i\sqrt{2}\theta_+}$, as ϕ_- is locked at $\langle\sqrt{2}\phi_-\rangle = \pi/2 \mod \pi$. These correlation functions show QLRO,

$$\langle O_{\mathrm{CDW}^\pi}(x) O^\dagger_{\mathrm{CDW}^\pi}(0)\rangle \sim x^{-K_+} e^{i2k_F x}, \tag{A15a}$$

$$\langle O_{\mathrm{SC}^d}(x) O^\dagger_{\mathrm{SC}^d}(0)\rangle \sim x^{-1/K_+}. \tag{A15b}$$

The dominant correlation is determined by the value of the TLL parameter K_+; the CDW (SC^d) state becomes most dominant for $K_+ < 1$ ($K_+ > 1$), i.e., $g + g' > 0$ ($g + g' < 0$).

For $K_- > 1$ (i.e., $g < g'$), the relevant order parameters are given by $O_{\mathrm{OAF}}(x) \to e^{i2k_F x - i\sqrt{2}\phi_+}$ and $O_{\mathrm{SC}^s}(x) \to e^{i\sqrt{2}\theta_+}$, and their correlation functions are

$$\langle O_{\mathrm{OAF}}(x) O^\dagger_{\mathrm{OAF}}(0)\rangle \sim x^{-K_+} e^{i2k_F x}, \tag{A16a}$$

$$\langle O_{\mathrm{SC}^s}(x) O^\dagger_{\mathrm{SC}^s}(0)\rangle \sim x^{-1/K_+}. \tag{A16b}$$

The dominant correlation is the OAF (SC^s) state when $K_+ < 1$ ($K_+ > 1$), i.e., $g + g' > 0$ ($g + g' < 0$).

Since the RG analysis described above correctly reproduces the phase diagram obtained in Ref. [38], the validity of our method is confirmed. As we noted earlier, the sinusoidal potentials of the two-chain Hamiltonian (A3) have forms similar to those of Eqs. (5.4). We can thus study the phase diagram of our model using the same RG method (with straightforward generalization), as described in Secs. IV and V, where the RG equations (4.4) are indeed similar to Eqs. (A14).

APPENDIX B: MAPPING TO TWO-COUPLED CHAIN WITH GAUGE FIELD

The model Hamiltonian (2.1) can be mapped to the Hamiltonian for the two-coupled chain with gauge field. By applying the phase representation only for the boson [Eq. (3.2a)], and by expressing $\Psi_f \to \Psi_1$ and $\Psi_\psi \to \Psi_2$, the effective Hamiltonian is expressed as

$$\begin{aligned} H_{f\psi} &\equiv H_f + H_\psi \\ &= \sum_{s=1,2} \int dx\, iu\left(\Psi_s^{L\dagger}\partial_x\Psi_s^L - \Psi_s^{R\dagger}\partial_x\Psi_s^R\right) \\ &\quad + \sum_{s=1,2} g\int dx \rho_s(x)\rho_s(x+\delta), \end{aligned} \tag{B1}$$

$$H_b = \frac{u}{2\pi}\int dx \left[\frac{1}{K_b}(\partial_x\phi_b)^2 + K_b(\partial_x\theta_b)^2\right], \tag{B2}$$

$$H_{3p} = -t_\perp \sum_{p=L,R}\int dx\left(\Psi_1^{p\dagger}\Psi_2^p e^{-i\theta_b} + \mathrm{H.c.}\right), \tag{B3}$$

where $t_\perp \equiv -g_{3p}/(2\pi\alpha)^{1/2}$, and we have set $u_b = u_f = u_\psi\ (\equiv u)$. We assumed the short-range interaction $V_{ff}(x - x') = g_f\delta(x - x' \pm \delta)$ and $V_{\psi\psi}(x - x') = g_\psi\delta(x - x' \pm \delta)$, where δ is the small quantity, and we set $g_f = g_\psi\ (\equiv g)$ for simplicity. We focus on the commensurate case $\rho_f = \rho_\psi$.

This model can be interpreted as the two-coupled chain model with a gauge field on the *rung*. In this section, we first eliminate the effect of the gauge field by gauge transformation and diagonalize the $t_\perp$ term. In the next step, we apply the bosonization, as performed in the two-chain problem [38]. By the gauge transformation

$$\Psi_1^p(x) \to \tilde{\Psi}_1^p(x) = \Psi_1^p(x)\, e^{+i\theta_b(x)/2}, \tag{B4}$$

$$\Psi_2^p(x) \to \tilde{\Psi}_2^p(x) = \Psi_2^p(x)\, e^{-i\theta_b(x)/2}, \tag{B5}$$

the $t_\perp$ term becomes $-t_\perp\sum_p\int dx(\tilde{\Psi}_1^{p\dagger}\tilde{\Psi}_2^p + \mathrm{H.c.})$. Since the $t_\perp$ term is expressed in the form of conventional interchain hopping, we can follow the approach of Ref. [38] in which the relevant $t_\perp$ term was treated nonperturbatively.

The interchain hopping term can be diagonalized by introducing the bonding and antibonding operators,

$$\Psi_+^p = \frac{1}{\sqrt{2}}\left(\tilde{\Psi}_1^p + \tilde{\Psi}_2^p\right), \quad \Psi_-^p = \frac{1}{\sqrt{2}}\left(\tilde{\Psi}_1^p - \tilde{\Psi}_2^p\right). \tag{B6}$$

The $t_\perp$ term is given by $-t_\perp\sum_p\int dx(\Psi_+^{p\dagger}\Psi_+^p - \Psi_-^{p\dagger}\Psi_-^p)$, and the intrachain kinetic terms are given by

$$\begin{aligned} &\int dx\, iu(\Psi_+^{L\dagger}\partial_x\Psi_+^L - \Psi_+^{R\dagger}\partial_x\Psi_+^R) \\ &\quad + \int dx\, iu(\Psi_-^{L\dagger}\partial_x\Psi_-^L - \Psi_-^{R\dagger}\partial_x\Psi_-^R) \\ &\quad + \frac{u}{2}\int dx(\Psi_+^{L\dagger}\Psi_-^L - \Psi_+^{R\dagger}\Psi_-^R + \mathrm{H.c.})(\partial_x\theta_b). \end{aligned} \tag{B7}$$

In contrast to the $t_\perp$ term, which is given in a diagonalized form, the intrachain kinetic terms contain the gauge field and the field operators are given in the nondiagonalized form.

Now we bosonize the fields $\Psi_\pm$,

$$\Psi_\pm^p(x) = \frac{\xi_\pm}{\sqrt{2\pi\alpha}} e^{in[k_F x - \phi_\pm(x)] + i\theta_\pm(x)}, \tag{B8}$$

where $n = +(-)$ for $p = R(L)$. In order to simplify the notation, we further apply the simple transformation,

$$\tilde{\phi}_+ = \frac{1}{\sqrt{2}}(\phi_+ + \phi_-), \quad \tilde{\phi}_- = \frac{1}{\sqrt{2}}(\phi_+ - \phi_-), \tag{B9}$$

TABLE I. The average value of $\langle\sqrt{2}\tilde{\theta}_-\rangle$ and the corresponding order parameter, determined by the fixed point value of the relevant g_θ^*.

Fixed point	Average value	Order parameter
$g_\theta^* > 0$	$\langle\sqrt{2}\tilde{\theta}_-\rangle = \pi/2 \bmod \pi$	$\langle\sin\sqrt{2}\tilde{\theta}_-\rangle \neq 0$
$g_\theta^* < 0$	$\langle\sqrt{2}\tilde{\theta}_-\rangle = 0 \bmod \pi$	$\langle\cos\sqrt{2}\tilde{\theta}_-\rangle \neq 0$

and then the Hamiltonians $H_{f\psi}$ and H_{3p} are expressed as

$$\begin{aligned} H_{f\psi} &= \frac{u_+}{2\pi}\int dx\left[\frac{1}{K_+}(\partial_x\tilde{\phi}_+)^2 + K_+(\partial_x\tilde{\theta}_+)^2\right] \\ &\quad + \frac{u_-}{2\pi}\int dx\left[\frac{1}{K_-}(\partial_x\tilde{\phi}_-)^2 + K_-(\partial_x\tilde{\theta}_-)^2\right] \\ &\quad - \frac{ig_0}{\pi\alpha}\int dx\,(\partial_x\theta_b)\sin\sqrt{2}\tilde{\theta}_-\cos\sqrt{2}\tilde{\phi}_- \\ &\quad + \frac{1}{2\pi^2\alpha^2}\int dx[-g_\phi\cos 2\sqrt{2}\tilde{\phi}_- + g_\theta\cos 2\sqrt{2}\tilde{\theta}_-], \\ H_{3p} &= t_\perp\int dx\frac{\sqrt{2}}{\pi}\partial_x\tilde{\phi}_-, \end{aligned} \tag{B10}$$

where

$$g_0 = u, \quad g_\phi = g_\theta = g[1-\cos(2k_F\delta)], \tag{B11}$$

and $K_\pm$ and $u_\pm$ depend on g and u. The microscopic determination of the parameters $K_\pm$ and $u_\pm$ are given in Ref. [38] for weak-coupling region, while it requires numerical analysis in the wide range of interactions.

From the scaling analysis, the RG equation for g_0 is given by $dg_0/dl = (1 - K_-/2 - K_-^{-1}/2)g_0$, implying that the g_0 term is marginal for $K_- = 1$ and becomes irrelevant for $K_- \neq 1$. The presence of the marginal or irrelevant g_0 term would give rise to slight renormalization of other quantities like K_b, K_-, g_ϕ, g_θ, and $t_\perp$. However, we argue below that, up to such relatively unimportant corrections, we can safely neglect the g_0 term so this Hamiltonian takes on the same form as two-coupled chains, derived in Ref. [38]. First, we observe that the $t_\perp$ term suppresses the potential $\cos 2\sqrt{2}\tilde{\phi}_-$, since the former favors the incommensurate state while the latter favors the commensurate state. Depending on the value of K_-, the $\tilde{\theta}_-$ field can either remain massless or develop a gap. We concentrate here on the case where $\tilde{\theta}_-$ develops a gap and acquires a nonzero expectation value determined by minimizing the ground-state energy. The average value of the massive field $\langle\sqrt{2}\tilde{\theta}_-\rangle$ depends on the sign of g_θ^*, where g_θ^* is the fixed-point value of g_θ. The average value of $\langle\sqrt{2}\tilde{\theta}_-\rangle$ and the corresponding order parameters are summarized in Table I.

The order parameters of the interest are $\mathcal{O}^{\rm DW}_{f\psi}$ [Eq. (3.5d)], $\mathcal{O}^{\rm SF}_{f\psi}$ [Eq. (3.5h)], and $\mathcal{O}^{\rm SF}_{bff+b^\dagger\psi\psi}$ [Eq. (3.5i)]. After the gauge transformation and the bosonization, these order parameters are written as

$$\begin{aligned} \mathcal{O}^{\rm DW}_{f\psi}(x) &= \Psi_1^{L\dagger}\Psi_1^R - \Psi_2^{L\dagger}\Psi_2^R \\ &= \tilde{\Psi}_1^{L\dagger}\tilde{\Psi}_1^R - \tilde{\Psi}_2^{L\dagger}\tilde{\Psi}_2^R \\ &= \Psi_+^{L\dagger}\Psi_-^R + \Psi_-^{L\dagger}\Psi_+^R \\ &= \frac{1}{\pi\alpha}e^{+i2k_Fx - i\sqrt{2}\tilde{\phi}_+}\sin\sqrt{2}\tilde{\theta}_-, \end{aligned} \tag{B12a}$$

$$\begin{aligned} \mathcal{O}^{\rm SF}_{f\psi}(x) &= \Psi_1^L\Psi_2^R + \Psi_2^R\Psi_1^L \\ &= \tilde{\Psi}_1^L\tilde{\Psi}_2^R + \tilde{\Psi}_2^L\tilde{\Psi}_1^R \\ &= \Psi_+^L\Psi_+^R - \Psi_-^L\Psi_-^R \\ &= \frac{1}{\pi\alpha}e^{i\sqrt{2}\tilde{\theta}_+}\sin\sqrt{2}\tilde{\theta}_-, \end{aligned} \tag{B12b}$$

$$\begin{aligned} \mathcal{O}^{\rm SF}_{bff+b^\dagger\psi\psi}(x) &= \frac{1}{\sqrt{2\pi\alpha}}\left(e^{i\theta_b}\,\Psi_1^L\Psi_1^R + e^{-i\theta_b}\,\Psi_2^L\Psi_2^R\right) \\ &= \frac{1}{\sqrt{2\pi\alpha}}\left(\tilde{\Psi}_1^L\tilde{\Psi}_1^R + \tilde{\Psi}_2^L\tilde{\Psi}_2^R\right) \\ &= \frac{1}{\sqrt{2\pi\alpha}}\left(\Psi_+^L\Psi_+^R + \Psi_-^L\Psi_-^R\right) \\ &= \frac{-2i}{(2\pi\alpha)^{3/2}}e^{i\sqrt{2}\tilde{\theta}_+}\cos\sqrt{2}\tilde{\theta}_-, \end{aligned} \tag{B12c}$$

where we have set $\xi_+\xi_- = i$.

When $g_\theta^* > 0$ (see Table I), we find that the correlation functions for $\mathcal{O}^{\rm DW}_{f\psi}$ and $\mathcal{O}^{\rm SF}_{f\psi}$ exhibit algebraic decay,

$$\left\langle\mathcal{O}^{\rm SF}_{f\psi}(x)\,\mathcal{O}^{\rm SF}_{f\psi}(0)^\dagger\right\rangle \sim x^{-1/K_+}, \tag{B13a}$$

$$\left\langle\mathcal{O}^{\rm DW}_{f\psi}(x)\,\mathcal{O}^{\rm DW}_{f\psi}(0)^\dagger\right\rangle \sim x^{-K_+}e^{i2k_Fx}. \tag{B13b}$$

This behavior is consistent with Eqs. (5.14) if we equate K_+ with K_2. We note that, in the simplified case where $u_b = u_f = u_\psi$ and $K_f = K_\psi$, the exponent K_2 is given by $K_2 \to K_f$, as seen from Eq. (5.14c).

On the other hand, when $g_\theta^* < 0$, the correlation function of $\mathcal{O}^{\rm SF}_{bff+b^\dagger\psi\psi}$ exhibits algebraic decay,

$$\left\langle\mathcal{O}^{\rm SF}_{bff+b^\dagger\psi\psi}(x)\,\mathcal{O}^{\rm SF}_{bff+b^\dagger\psi\psi}(0)^\dagger\right\rangle \sim x^{-1/K_+}. \tag{B14}$$

This behavior is consistent with Eq. (5.15b) by noting that the exponent $\eta_{\vartheta 2}$ is given by $\eta_{\vartheta 2} \to 1/K_f$ [Eqs. (5.16)] in the case of $u_b = u_f = u_\psi$ and $K_f = K_\psi$.

[1] H. Feshbach, Ann. Phys. **5**, 357 (1958).

[2] C. A. Regal, M. Greiner, and D. S. Jin, Phys. Rev. Lett. **92**, 040403 (2004).

[3] M. W. Zwierlein, C. A. Stan, C. H. Schunck, S. M. F. Raupach, A. J. Kerman, and W. Ketterle, Phys. Rev. Lett. **92**, 120403 (2004).

[4] J. Kinast, S. L. Hemmer, M. E. Gehm, A. Turlapov, and J. E. Thomas, Phys. Rev. Lett. **92**, 150402 (2004).

[5] C. Chin, M. Bartenstein, A. Altmeyer, S. Riedl, S. Jochim, J. H. Denschlag, and R. Grimm, Science **305**, 1128 (2004).

[6] I. Bloch, J. Dalibard, and W. Zwerger, Rev. Mod. Phys. **80**, 885 (2008).

[7] C. Pethick and H. Smith, *Bose-Einstein Condensation in Dilute Gases*, 2nd ed. (Cambridge University Press, Cambridge, 2008).

[8] S. J. J. M. F. Kokkelmans, J. N. Milstein, M. L. Chiofalo, R. Walser, and M. J. Holland, Phys. Rev. A **65**, 053617 (2002).

[9] G. M. Bruun and C. J. Pethick, Phys. Rev. Lett. **92**, 140404 (2004).
[10] O. Dulieu and C. Gabbanini, Rep. Prog. Phys. **72**, 086401 (2009).
[11] C. A. Stan, M. W. Zwierlein, C. H. Schunck, S. M. F. Raupach, and W. Ketterle, Phys. Rev. Lett. **93**, 143001 (2004).
[12] S. Inouye, J. Goldwin, M. L. Olsen, C. Ticknor, J. L. Bohn, and D. S. Jin, Phys. Rev. Lett. **93**, 183201 (2004).
[13] H. Yabu, Y. Takayama, and T. Suzuki, Physica B **329-333**, 25 (2003).
[14] H. Yabu, Y. Takayama, T. Suzuki, and P. Schuck, Nucl. Phys. A **738**, 273 (2004).
[15] S. K. Adhikari, Phys. Rev. A **70**, 043617 (2004).
[16] S. Powell, S. Sachdev, and H. P. Büchler, Phys. Rev. B **72**, 024534 (2005).
[17] D. B. M. Dickerscheid, D. van Oosten, E. J. Tillema, and H. T. C. Stoof, Phys. Rev. Lett. **94**, 230404 (2005).
[18] J. Zhang and H. Zhai, Phys. Rev. A **72**, 041602(R) (2005).
[19] A. V. Avdeenkov, D. C. E. Bortolotti, and J. L. Bohn, Phys. Rev. A **74**, 012709 (2006).
[20] D. C. E. Bortolotti, A. V. Avdeenkov, and J. L. Bohn, Phys. Rev. A **78**, 063612 (2008).
[21] S. Akhanjee, Phys. Rev. B **82**, 075138 (2010).
[22] M. A. Cazalilla, J. Phys. B **37**, S1 (2004).
[23] For a recent review, see M. A. Cazalilla, R. Citro, T. Giamarchi, E. Orignac, and M. Rigol, Rev. Mod. Phys. **83**, 1405 (2011).
[24] M. A. Cazalilla and A. F. Ho, Phys. Rev. Lett. **91**, 150403 (2003).
[25] L. Mathey, D.-W. Wang, W. Hofstetter, M. D. Lukin, and E. Demler, Phys. Rev. Lett. **93**, 120404 (2004).
[26] L. Mathey and D.-W. Wang, Phys. Rev. A **75**, 013612 (2007).
[27] I. Danshita and L. Mathey, Phys. Rev. A **87**, 021603(R) (2013).
[28] E. Orignac, M. Tsuchiizu, and Y. Suzumura, Phys. Rev. A **81**, 053626 (2010).
[29] D. E. Sheehy and L. Radzihovsky, Phys. Rev. Lett. **95**, 130401 (2005).
[30] E. Orignac and R. Citro, Phys. Rev. A **73**, 063611 (2006).
[31] K. K. Das, Phys. Rev. Lett. **90**, 170403 (2003).
[32] L. Pollet, M. Troyer, K. Van Houcke, and S. M. A. Rombouts, Phys. Rev. Lett. **96**, 190402 (2006).
[33] T. Giamarchi, *Quantum Physics in One Dimension* (Oxford University Press, Oxford, 2003).
[34] F. M. Marchetti, T. Jolicoeur, and M. M. Parish, Phys. Rev. Lett. **103**, 105304 (2009).
[35] A. A. Nersesyan, A. Luther, and F. V. Kusmartsev, Phys. Lett. A **176**, 363 (1993).
[36] A. O. Gogolin, A. A. Nersesyan, and A. M. Tsvelik, *Bosonization and Strongly Correlated Systems* (Cambridge University Press, Cambridge, 1998).
[37] V. M. Yakovenko, JETP Lett. **56**, 510 (1992).
[38] E. Orignac and T. Giamarchi, Phys. Rev. B **56**, 7167 (1997).
[39] J. Kogut, Rev. Mod. Phys. **51**, 659 (1979).
[40] T. Ohta and D. Jasnow, Phys. Rev. B **20**, 139 (1979).
[41] P. Nozieres and F. Gallet, J. Phys. France **48**, 353 (1987).
[42] K. A. Muttalib and V. J. Emery, Phys. Rev. Lett. **57**, 1370 (1986).
[43] U. Ledermann and K. Le Hur, Phys. Rev. B **61**, 2497 (2000).
[44] R. Folman, P. Kruger, J. Schmiedmayer, J. Denschlag, and C. Henkel, Adv. At. Mol. Opt. Phys. **48**, 263 (2002).
[45] S. Hofferberth, I. Lesanovsky, T. Schumm, A. Imambekov, V. Gritsev, E. Demler, and J. Schmiedmayer, Nat. Phys. **4**, 489 (2008).
[46] L. Mathey, E. Altman, and A. Vishwanath, Phys. Rev. Lett. **100**, 240401 (2008).
[47] K. Mølmer, Phys. Rev. Lett. **80**, 1804 (1998).
[48] A. Recati, P. O. Fedichev, W. Zwerger, and P. Zoller, Phys. Rev. Lett. **90**, 020401 (2003); J. Opt. B **5**, S55 (2003).
[49] G. G. Batrouni, V. Rousseau, R. T. Scalettar, M. Rigol, A. Muramatsu, P. J. H. Denteneer, and M. Troyer, Phys. Rev. Lett. **89**, 117203 (2002).
[50] C. Kollath, U. Schollwöck, J. von Delft, and W. Zwerger, Phys. Rev. A **69**, 031601(R) (2004).
[51] S. Fölling, A. Widera, T. Müller, F. Gerbier, and I. Bloch, Phys. Rev. Lett. **97**, 060403 (2006).